Dybdeoplysningerne er fjernet!!!

Extension of the Naval station Korsor

Hydrodynamic model simulation of the sediment spill from dredging

SWECO

Sweco Sverige AB	Reg. No. 556767-9849
Project Name	FES_BHR_Flådestation_Korsør_2025
Project Number	41012234-056
Client	Forsvarsministeriets Ejendomsstyrelse - FES
Author	Jurjen de Jong, Piotr de Bever
Controlled by	Emanuel Schmidt
Date	2025-12-02
Document reference	Hydrodynamic modelling of sediment spill from dredging - Naval port Korsor_v20251202.docx
Front page	Suspended sediment from mooring operation 2023-03-04 (source: Skråfoto Klimadatastyrelsen)

Table of contents

1 General

1.1 Introduction

The Danish Armed Forces (*Forsvaret*) is planning to extend the naval station in Korsor (*Flådestation Korsør*). As part of this extension, the entire port will be dredged to a new depth and a new layout (see section 1.3). During the dredging, fine sediments will be spilled to the water and increase the suspended sediment concentrations and related dissolved substances. The impact on the environment is studied in relation to Water Framework Directive (WFD). This study is background material to the assessment of the WFD.

1.2 Goal and deliverables

This report uses a 3D hydrodynamic model to predict the currents and water levels in the Great Belt. This model is used to predict the transport of the sediment spill from the dredging of the port basins. The following model results are reported:

- The increase in total suspended sediment (TSS)
- The deposition of sediment
- The increase in concentrations of dissolved nutrients and MFS that are released during the dredging.

The interpretation of the reported findings is only limited in this report and further described in other appendices to the assessment of the WFD.

1.3 Dredging plan

Dredging of the port is being carried out in 2 stages. At first maintenance dredging is carried out where most of the existing port is dredged to a bed level of x m (see Figure 1.1). After the maintenance dredging, additional dredging will deepen both port basins. A land fill will be realised between the western and eastern basin (see Figure 1.2). A new breakwater will be constructed west of the breakwaters.

Of these activities, only the additional dredging for the deepening of the basins is part of the scope of this study. The total volume of dredged sediment is estimated at 154 948 m^3. This is a conservative estimate.

A sediment retention barrier (a bubble barrier or silt curtain) could be used during the dredging, which could reduce concentrations of suspended sediment and dissolved substances.

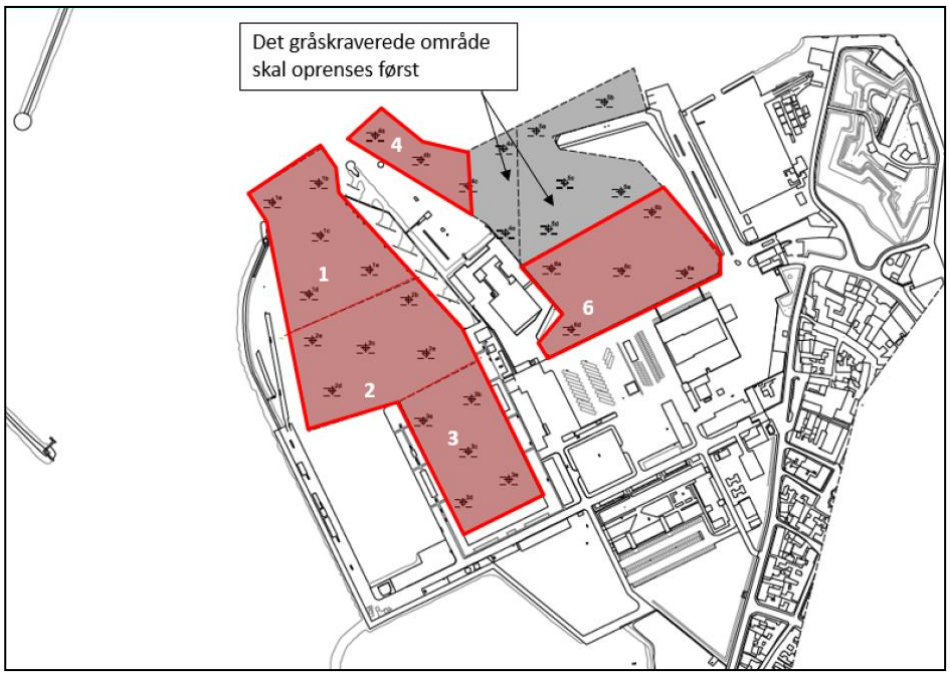

Figure 1.1: Area of maintenance dredging (not part of the project). Both the grey and red areas are dredged to a bed level at x m.

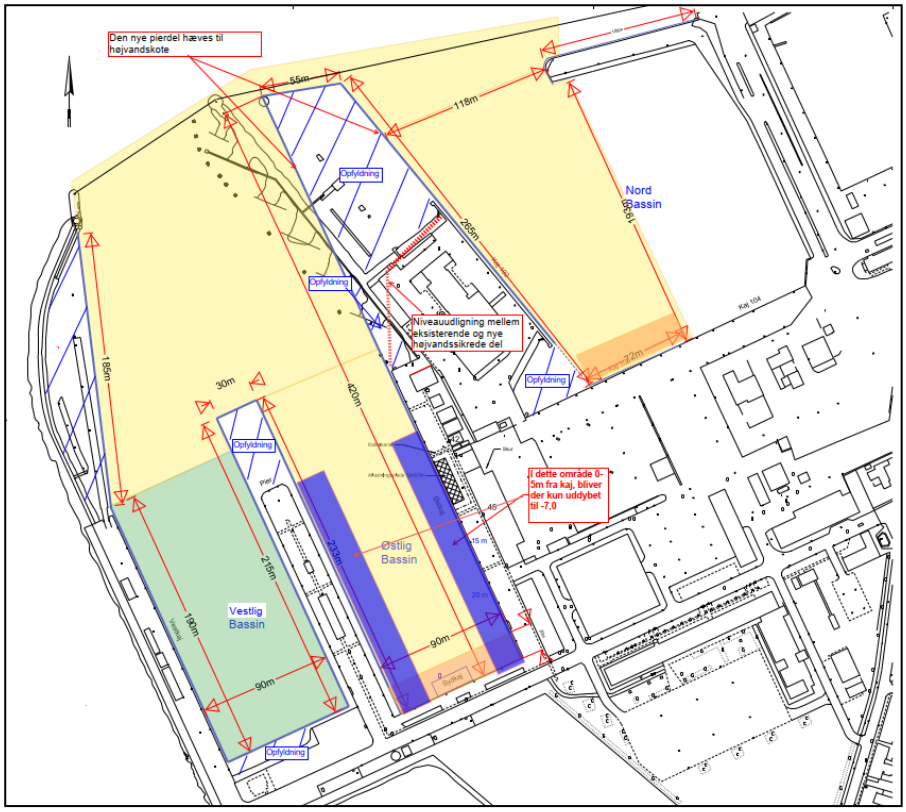

Figure 1.2: Dredging plan, part of the project scope.

1.4 Supporting data

An overview of all the data that is used in model setup and validation is given in Table 1.1.

Table 1.1: Overview of data used in the model setup and model validation.

#	Data	Description	Source
[1]	Bathymetry	EMODnet Bathymetry DTM 2024 (resolution of 1/16 arc minutes, ca. 115 m) https://doi.org/10.12770/cf51df64-56f9-4a99-b1aa-36b8d7b743a1	EMODnet
[2]	Bathymetry	Danmarks Dybdemodel (DDM) (resolution of 50 m) https://dataforsyningen.dk/data/4817	Geodatastyrelsen
[3]	Bathymetry	High resolution data around the port Korsor • 2302059_Korsør_DTM (point cloud) • Korsør Havn - Opmåling - 2020 (raster)	*Client*
[4]	Salinity and Temperature	Measurements by the BSH (Das Bundesamt für Seeschifffahrt und Hydrographie). Analyses and validation at station Fehmarn Belt Buoy (6600023) which measures over the full depth at every hour.	Copernicus Marine Service
[5]	Velocities	Measurements at Great Belt Bridge East CU and Vengeance CU, used for validation of the velocities. Measured by FOCO	Copernicus Marine Service
[6]	Water level	Observations of water levels at 10-minute interval. Stations used for model setup: Århus, Rodbyhavn.	DMI
[7]	Wind	Hourly averaged wind speed at stations: Røsnæs Fyr, Omø Fyr, Langø, Assens/Torø	DMI
[8]	Model results of velocity, salinity and temperature	Model results from the Baltic Sea Physics Reanalyses (Nemo-Nordic) for the period 2022-05-01 – 2023-05-01. Results cover the entire area of this reports model and contain salinity, temperature, velocities and water levels at a resolution of 1 nautical mile (1852 meter) at a daily timestep. https://doi.org/10.48670/moi-00013	Copernicus
[9]	Geotechnical and environmental data	Analyse rapport of preliminary results of the analyses of 6 measurement. This data contains TotP and TotN, and sieve curves for all points. June and July 2025. 41012234-056,133457-133462-25 07-07-2025 10.54.08-928 V 2.pdf PR2571264_0_COA_Standard_CAI.pdf PR2571264_Attachment_1.pdf PR2571264_Attachment_2.pdf	ALS Denmark A
[10]	Drilling profiles	Assembly of drilling profiles of both western and eastern basin. Based on earlier measurements from 25188 (25 profiles from 2004 and 2005) and 5275 (6 profiles from 1952, 1953 and 1960). Additionally, 24 new drillings were carried out in 2025. Dated 2025-06-23. 209590_R1.pdf	Geo Subsurface expertise
[11]	Environmental data	Analyses of substances for 14 samples that were taken from the drillings in 2025 [10]. Korsør Flådestation - Geo sag 209590_Rapport 2_Miljøundersøgelse.pdf	Geo Subsurface expertise ALS Denmark A

2 Background

2.1 Hydrodynamics in the Danish Straits

The Danish Straits form a system of water passages connecting Baltic Sea with North Sea, comprising Kattegat, Oresund, Great Belt, and Little Belt (Figure 2.2). These straits play a crucial role in the exchange of water between the Baltic Sea and the ocean, enabling both the inflow of saline water from the North Sea and the outflow of less saline Baltic water. This exchange is stratified and influenced by density gradients, tides, and meteorological conditions.

The modelled domain includes Great Belt and Little Belt, two parallel straits located between the Jutland peninsula and the islands of Funen and Zealand. These straits are important for water mass transport between Kattegat and Baltic Sea. In Kattegat, surface salinity can reach 30 PSU, while the outflowing Baltic waters typically have salinity levels around 10 PSU. These differences result in stratification, with fresher Baltic water flowing in the upper layers and denser North Sea water entering in the lower layers. The yearly variation in stratification of salt and temperature at the Fehmarn Belt is shown in Figure 2.1 and shows the strongest change in density at a depth between 15 and 20 meters.

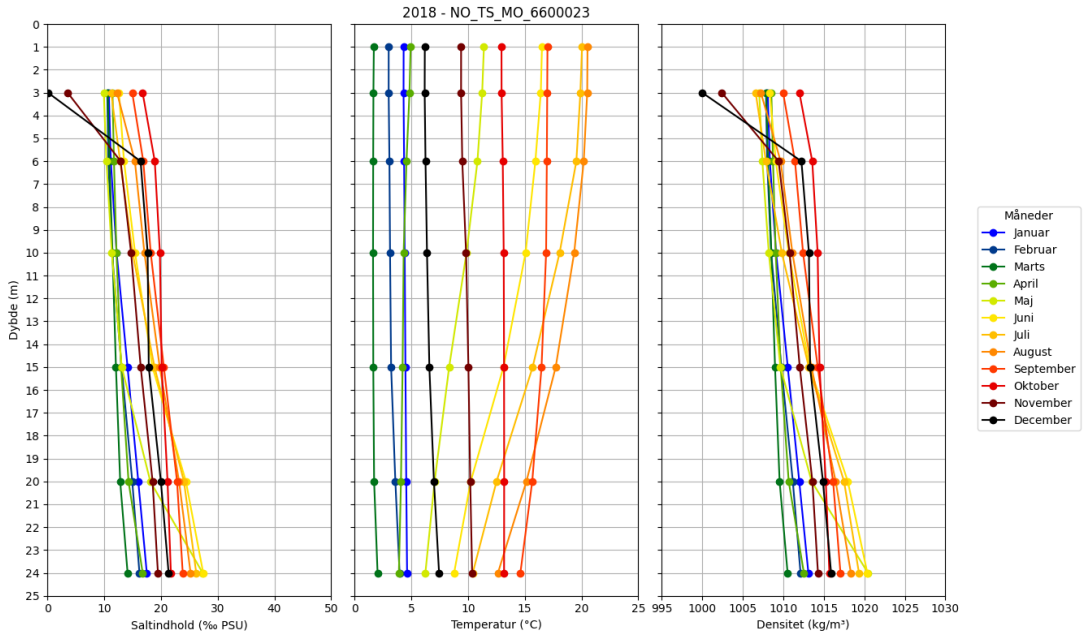

Figure 2.1: Measurements of salinity and temperature at station Fehmarn Belt Buoy in 2018 (data [4])

The seabed in Great and Little Belts is characterised by complex morphology, including a system of deep, elongated channels that play a vital role in water exchange. These erosional troughs, often exceeding 50 metres in depth, serve as primary pathways for the inflow of dense saline water from the Kattegat into the Baltic Sea.

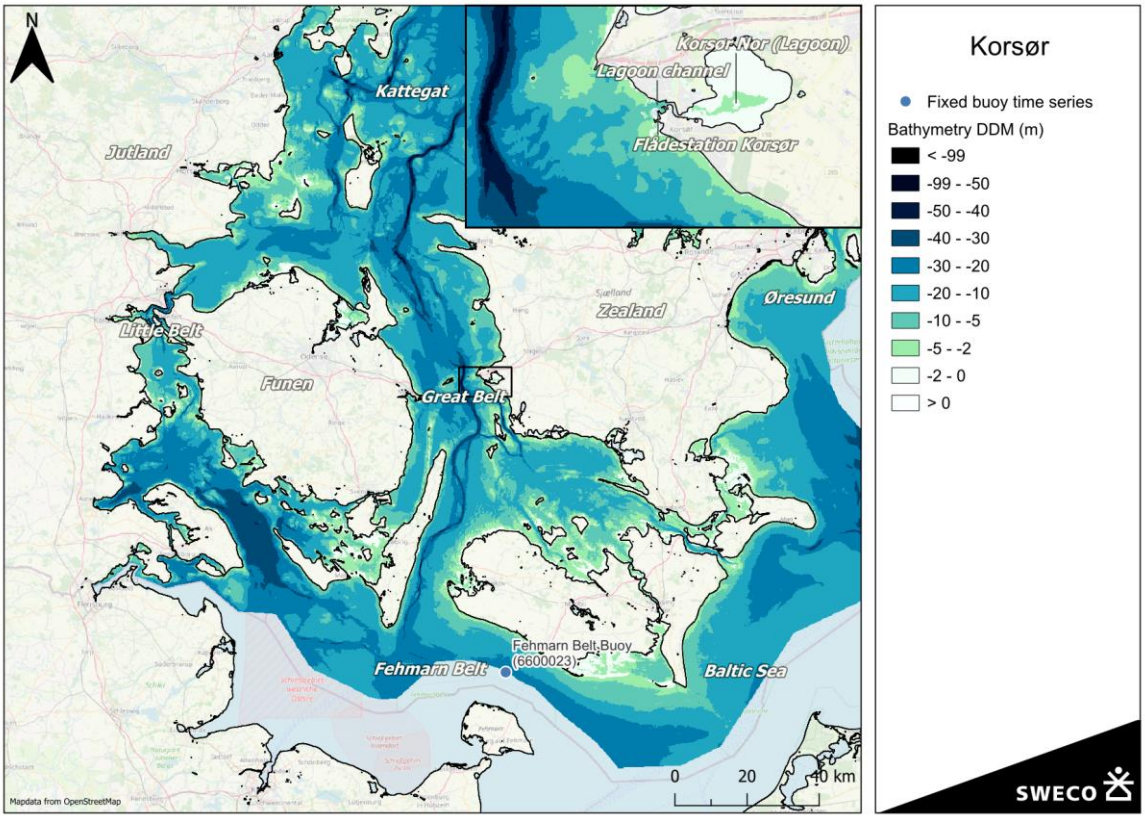

Figure 2.2: The Danish Straits, with a detail of the area around Korsor.

Water exchange between the North Sea and the Baltic occurs through two primary mechanisms: barotropic and baroclinic inflows.

- Barotropic inflows are driven by differences in sea surface elevation between Kattegat and Baltic Sea, which may result from tides, wind forcing, or atmospheric pressure gradients. In such cases, the flow is vertically uniform, with the entire water column moving in the same direction regardless of density. Larger events are called Major Baltic Inflows and are important for the environment in the Baltic Sea.
- Baroclinic inflows, on the other hand, are driven by density differences between the fresher Baltic water and the more saline North Sea water. These flows are stratified: the upper layers are dominated by the outflow of Baltic water, while the lower layers carry inflowing saline water. Baroclinic inflows are critical for the renewal of deep water in the Baltic Sea. Their intensity and frequency depend on meteorological conditions, seasonal variations in temperature and salinity, and the morphology of the straits.

The Naval Station Korsor is located at the Great Belt along a channel to the shallow lagoon Korsor Nor (Figure 2.2). This lagoon is classified by the WFD as a bay. The flow through this *lagoon channel* is dominated by a tidal current which is forced by the water level variation in the Great Belt. The average tidal range at measurement station Korsor is circa 0,5 m.

2.2 Representative period

The period that is used as forcing for the model has been selected to be a recent and representative period with good data availability. The data availability is limited by the regional hydrodynamic model (data [8]) and the available measurements on the currents at the Great Belt Bridge which were only available starting 2022-05-01. A full overview of data available at given periods is given in Appendix A. The period evaluated in the model starts thus also on 2022-05-01.

The chosen model period has further been evaluated as representative for the general dynamics of the area. The wind, water levels and Baltic Sea major inflow events are representative for an average year.

For the validation of the model the first 142 days are used. For the model application of dredging the first 91 days of this period are used: 2022-05-01 to 2022-07-31, as further explained in section 3.2.

Below a selection of forcing data for the selected periods is given. Figure 2.3 shows daily water levels, and Figure 2.4 the wind conditions. How these are included in the model is also explained in more detail in section 3.2.

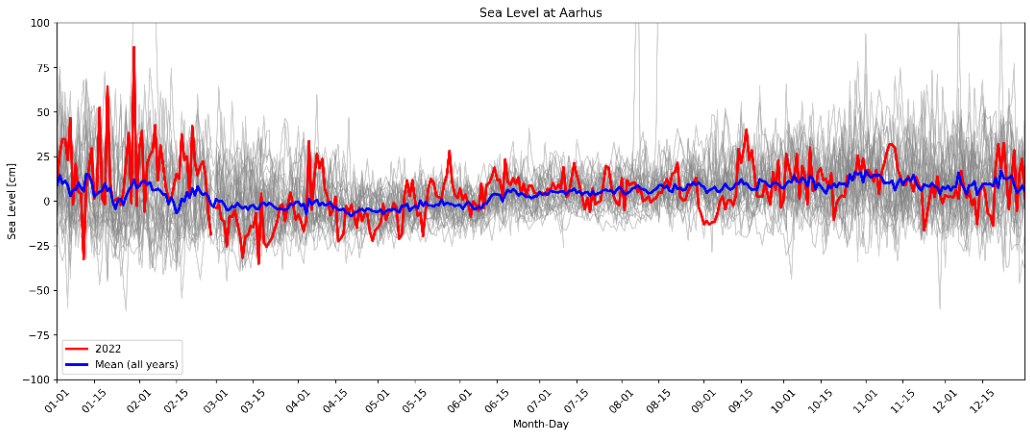

Figure 2.3: Daily average water levels (wind setup) at station Aarhus during the model validation period.

In the analysed period, wind conditions in the area of the measuring station were characterized by a clear dominance of westerly and south-westerly winds.

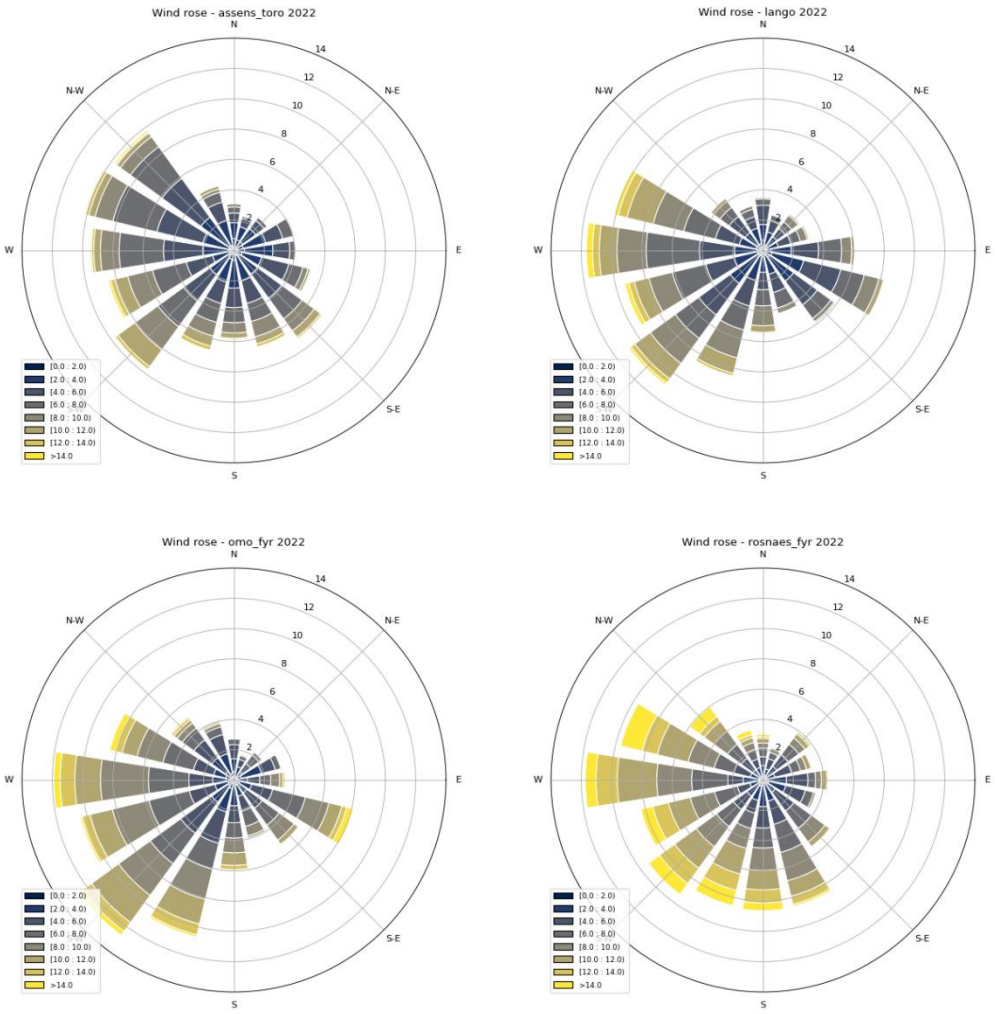

Figure 2.4: Wind roses for the year 2022 for 4 stations around the model area.

2.3 Sediment properties

The dredged sediment consists of a combination of sand, organic mud, clay and moraine. The composition of these fractions over the material that will be dredged, varies over 50 drilling profiles that are available within the western and eastern basin (data [10]). The dominant soil type in the drilling profiles are organic mud (gyttja) and clay. Additionally, a sieve analyses of 4 sediment samples within the western basin (data [9]) show a similar variability in sediment distribution, see Table 2.1 (locations as *Samples 1* in Figure 2.5).

A representative sediment distribution has been composed by taking a weighted average of the 4 samples. This weighting factor has been configured in a conservative way. It includes a large factor (0.6) for station 3 which is representative for the organic mud and clay that forms a large part of the dredged sediment. Lower emphasis has been attributed to station 4 since this is expected to be of shallow depth and not representative for all of the dredged sediment, thus the smaller fraction (0.2) for station 4.

The weighted sedimentation distribution has a fraction fine sediment, with a diameter below 125 µm, of 35%. The larger sediment fractions are excluded from the model because their high settling velocities cause them to remain in suspension for a short period. As a result, they are unlikely to be transported outside the dredging zone in port basins.

Table 2.1: Representative sediment distribution based on a weighted average of station 1, 3 and 4. These stations are named *Samples 1* in Figure 2.5.

	Clay and fine silt	Medium silt	Coarse Silt	Fine Sand	Larger factions	Weighting Factor
Diameter (µm)	< 6,3	6,3 - 20	20 - 63	63 - 125	> 125	
Station 1: 133457/25	2%	6%	5%	5%	83%	0.2
Station 2: 133458/25	0%	1%	1%	0%	98%	0
Station 3: 133459/25	5%	11%	9%	5%	70%	0.6
Station 4: 133460/25	7%	26%	26%	10%	31%	0.2
Weighted average	**5%**	**13%**	**12%**	**6%**	**65%**	

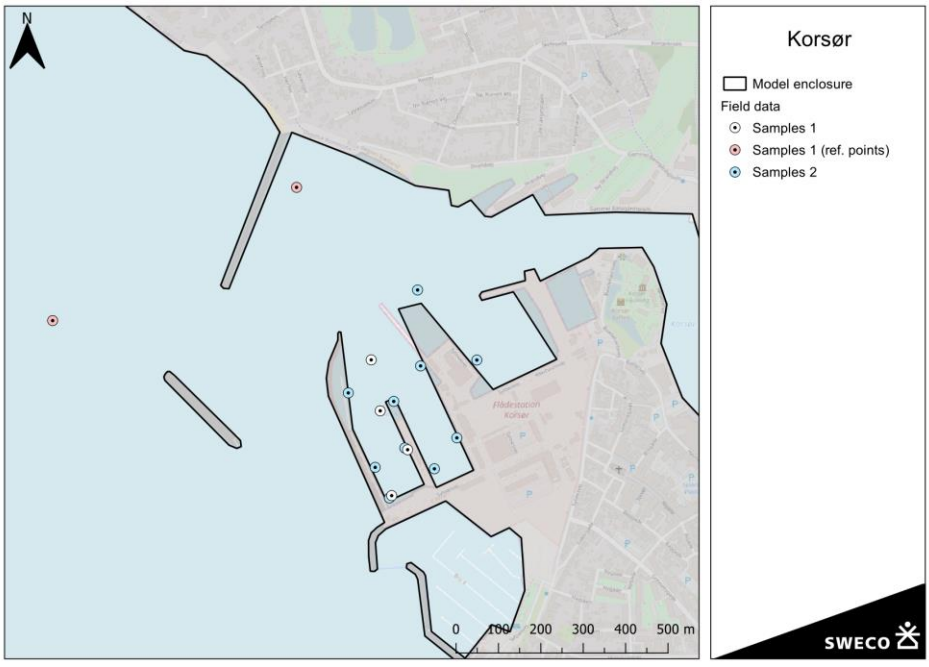

Figure 2.5: Location of the samples in both geotechnical analyses. Dataset 1 contain 4 samples in the basins and 2 reference samples outside the basins [9]. Dataset 2 contains 14 samples in and directly outside of the basins [11].

During the dredging, sediment-bound substances will be dissolved in the water and cause an increase in concentrations. Different methodology is applied for the spreading of nutrients and the spreading of environmentally hazardous substances (*miljøfarlige forurenende stoffer*, MFS).

Of the fraction of the dredged sediment that is suspended in the water column (sediment spill, see section 3.3), a fraction of the sediment-bound substances will be dissolved in the water. The method and assumptions are further explained in section 3.4. Sediment-bound concentrations and parameters used to calculate the dissolved fraction are given in Table 2.2 and Table 2.3.

Table 2.2: The sediment-bound concentration TN and TP, as the average of the 18 samples available within the basins [9] [11] (*Samples 1* and *Samples 2* in Figure 2.5). The dissolved fraction is the fraction that is released during the first day that sediment is suspended, based on measurements for gyttja (DHI, 2024). More on this in section 3.4.

Component	**Average of 18 samples (mg/kg)**	**Dissolved fraction**
Total nitrogen (TN)	1382	4,8%
Total phosphorus (TP)	514	6,5%

Table 2.3. Substances in the sediment as the average over the 14 samples [11] (*Samples 2* in Figure 2.5). The distribution coefficient Kd gives the equilibrium balance between dissolved and sediment-bound concentrations within a given control volume (Miljøstyrelsen, 2025). More on this in section 3.4. For each of the substances, the environmental quality standards (EQS) for the dissolved fraction is given (Miljøministeriet, 2003).

Component	Average of 14 samples (mg/kg)	Distribution coefficient log(Kd)	Environmental quality standards (µg/l)
Tungmetaller			
Arsen, As	5.5	1.92	2.6
Bly, Pb	13.3	5.47	1.3
Cadmium, Cd	0.3	5.11	0.2
Chrom (total), Cr	27.3	5.10	3.4
Kobber, Cu	31.8	4.39	1.2
Kviksølv, Hg */**	0.03	5.23	0.07
Nikkel, Ni	25.0	3.85	8.6
Zink, Zn	74.3	3.49	8
PAH'er			
Phenanthren	0.02	4.36	0.94
Antracen	0.02	4.46	0.1
Fluoranthen	0.0608	3.39	0.0063
Pyren	0.0706	4.77	0.0023
Benz(a)anthracen	0.0271	5.7	0.0005
Chrysen	0.0416	5.81	0.0014
Benz(a)pyren	0.03786	6.13	0.00017
Indeno(1,2,3-cd)pyren	0.03714	6.13	0.00017
Benz(ghi)perylen	0.04143	6.13	0.00017
Nonylphenoler	0.016	4.48	0.3
Methylnaphthalener, mono, di og tri	0.24	3.65	0.12
Sum af PFOA, PFOS, PFNA, PFHxS, høj LOD	0.001	3.3	0.00013

3 Method

3.1 Hydrodynamic modelling with Telemac

TELEMAC is a numerical modelling software maintained by the TELEMAC-MASCARET consortium. Originating in the 1990s, it has become one of the leading tools for simulating water flows in both riverine and marine environments, with particular strength in coastal and estuarine applications.

The TELEMAC-3D computational engine enables the simulation of three-dimensional, nonlinear free-surface flows, accounting for density variations, turbulence, and tidal effects. Calculations are performed using the finite element method on an unstructured triangular mesh, allowing for accurate representation of complex geometries such as straits, bays, and harbours.

The model is based on Navier-Stokes equations, solved in either hydrostatic or non-hydrostatic form. TELEMAC-3D allows for the transformation of a 2D model into a 3D one by defining vertical layers, enabling detailed representation of vertical velocity profiles and stratification processes.

In marine models such as the one discussed in this report, salinity and temperature variations play a crucial role. TELEMAC-3D supports modelling of these parameters as fields that influence water density, which in turn affects circulation patterns. In environments where thermal and salinity stratification occurs, a three-dimensional model is significantly more appropriate than a 2D approach, as it can capture vertical density gradients that influences flow direction, mixing processes, and mass and energy transport.

3.2 Model setup

The model uses a three-dimensional representation of flow, accounting for density-driven circulation, atmospheric forcing, and Coriolis effects. The model uses an unstructured mesh with the vertical described with 15 layers, enabling the simulation of thermal and salinity stratification and their influence on flow dynamics. Temperature and salinity are treated as active tracers, directly affecting water density and the resulting circulation patterns.

The geographical extent of the model has been chosen to include both the Great and Small Belt (Figure 3.1). By choosing a large extent, the model is expected to best calculate the velocities from the barotropic and baroclinic inflows. Boundaries are chosen where the sea is narrow for best model stability. Two open boundaries have been included: A northern boundary near Aarhus, and a south-eastern boundary at the Fehmarn Belt. These boundary conditions control water level, velocity, salinity and temperature. Water levels are taken from the nearby stations Rodbyhavn for the southern boundary and Aarhus at the northern boundary (data [6]). Other parameters are obtained from the Nemo-Nordic model (data [8]) of the Copernicus Programme.

The bathymetry in the model is primarily based on the DDM (data [2]). In areas not covered by DDM, bathymetry is used from EMODnet (data [1]). In the area around the Korsor the bathymetry has been improved using a recent bathymetric survey. To reduce the numerical diffusion and the flow resistance of the Belt Sea the model bathymetry has been smoothed. This increases the discharges through the Great Belt and improves stratification.

The new port layout and planned depth of the basins is included in the model. This means that both the land fill and dredging have already been realised. This is expected to be closest to the situation during dredging but is also not expected to have a noticeable effect on the model results. A proposed breakwater west of the port basins (not shown in this report) is expected to be constructed after the dredging and is not included in the model. This breakwater will impact the flows through the lagoon channel, but the expected impact on the dispersion of the sediment is small.

The impact of wind shear stress to the water surface is included. Wind measurements are obtained from four DMI meteorological stations (Røsnæs Fyr, Omø Fyr, Langø and Assens/Torø) and interpolated over the model domain. No correction factor has been applied for expected lower or higher wind velocities on open water.

The suspended sediment is modelled conservatively as non-cohesive sediment, and the sediment spill is further described in section 3.3. The model includes the settling velocities per sediment classes, deposition, advection and diffusive processes of the suspended matter and includes resuspension. In the sediment spill also a soluble inert unit tracer is included to monitor the transport of substances in the sediment.

The calculation period has been chosen different for the model validation and the model application. For the model validation a period of 142 days is modelled, starting 2022-05-01. For the model application for studying the dredging impact a period of 91 days is chosen starting on 2022-05-01, of which the first 2 days are intended for stabilising the initial conditions, 59 days are used for dredging work (see section 3.3), and the remaining period for the transport and settling of the sediment.

Model results are presented in different parts of the water column. Results at the *bed*, are the average of the deepest 1 m in the water column. Model results at the *surface* are the average of the 1 m directly below the water surface. Other maps show depth-average results, which is also the case if bed nor surface is specified.

For maps of maxima, hourly fluctuations are not representative for the environmental impact. Model results have therefor been averaged over periods of 6 hours before taking the maximum over the model period. In the study of increased concentrations of substances, results are resampled to daily averages.

In the validation of model results, metrics and model performance criteria are selected as described in Appendix B.

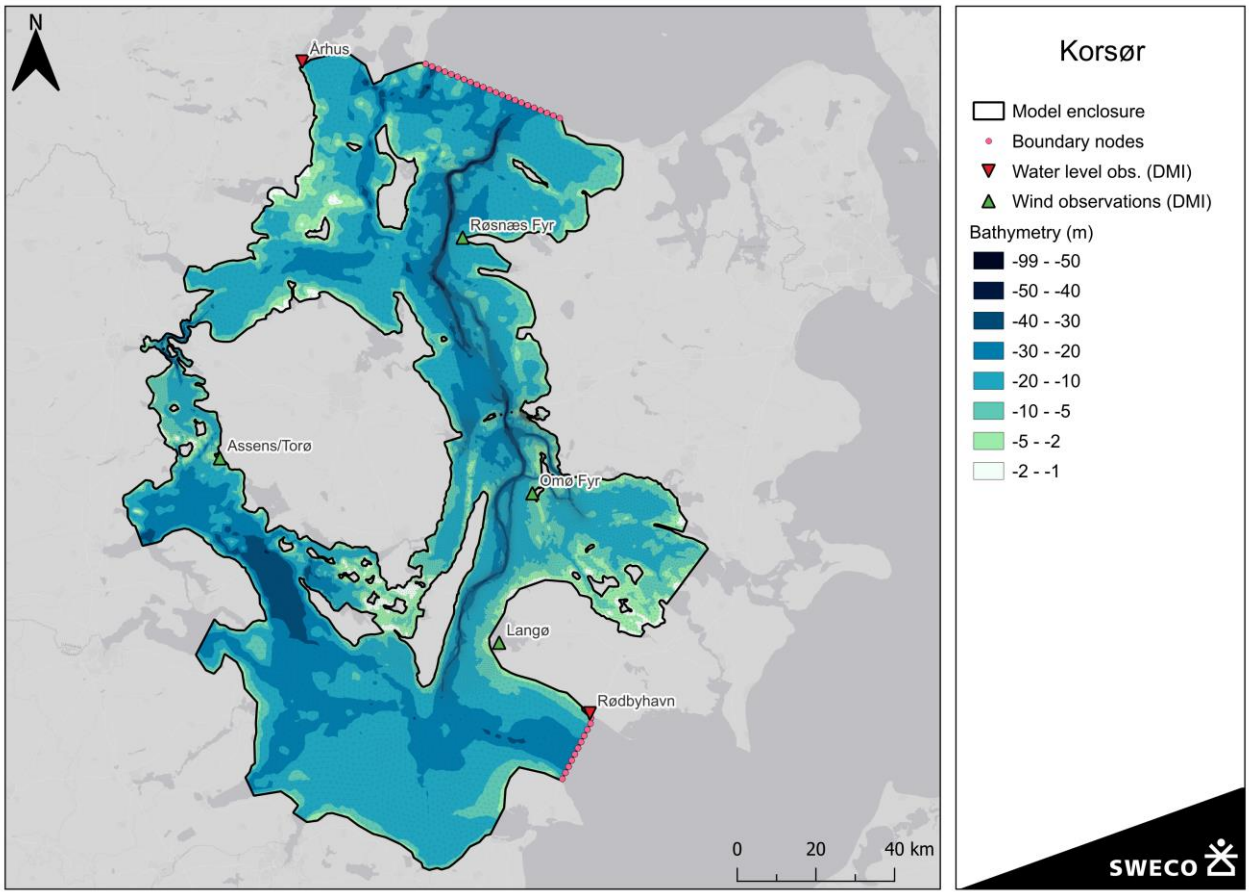

Figure 3.1: Overview of the model. Including the water level stations that are used on the open model boundaries, the wind stations that are interpolated which are used to model wind stress, and the boundary nodes at which data from Nemo-Nordic is applied.

3.3 Sediment spill modelling

It is assumed that the dredging will be carried out using a Grab dredger, which is the same technique as currently used for the maintenance dredging. Dredging will be carried out 12 hours a day, 7 days a week. Using a production rate for the grab dredger of 220 m^3/hour (equal to 97 kg/s), the dredging is expected to take 59 days. In the model this is applied on subsequent days, which results in higher concentrations than if the dredging is carried out over a longer period. As the spreading of sediment spill comes predominantly from the tidal currents, it is not expected to be different during other seasons.

In the model, the dredging is modelled at representative points over the dredged area (Figure 3.3). The dredger moves every 5 days to the next point. A time series of this dredging process is shown in Figure 3.2 for the first 3 weeks of the model.

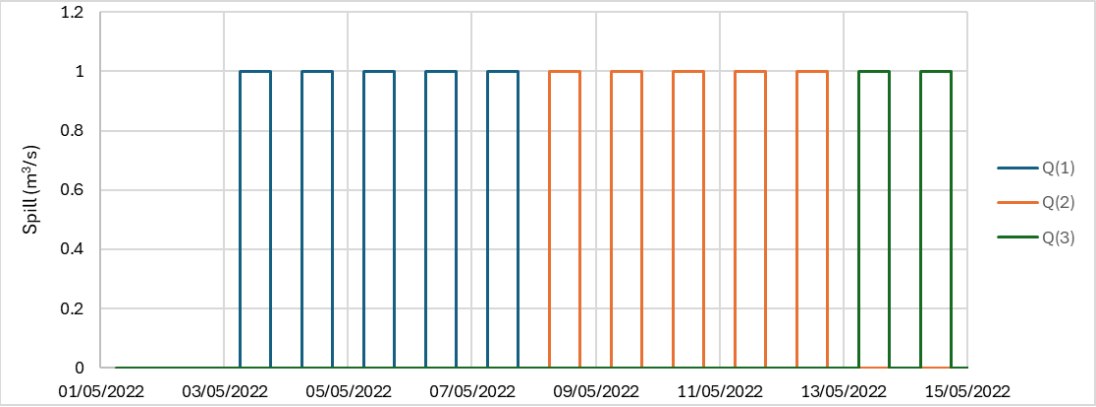

Figure 3.2: Example of the sediment spill in the first 3 weeks of the simulation. After an initial initialisation of 2 days, the sediment spill moves every 5 days to a new point within the dredged area. The quantity (1 m^3/s) indicates the spill as modelled by a sediment slurry, the sediment fractions within this slurry are specified in Table 3.1.

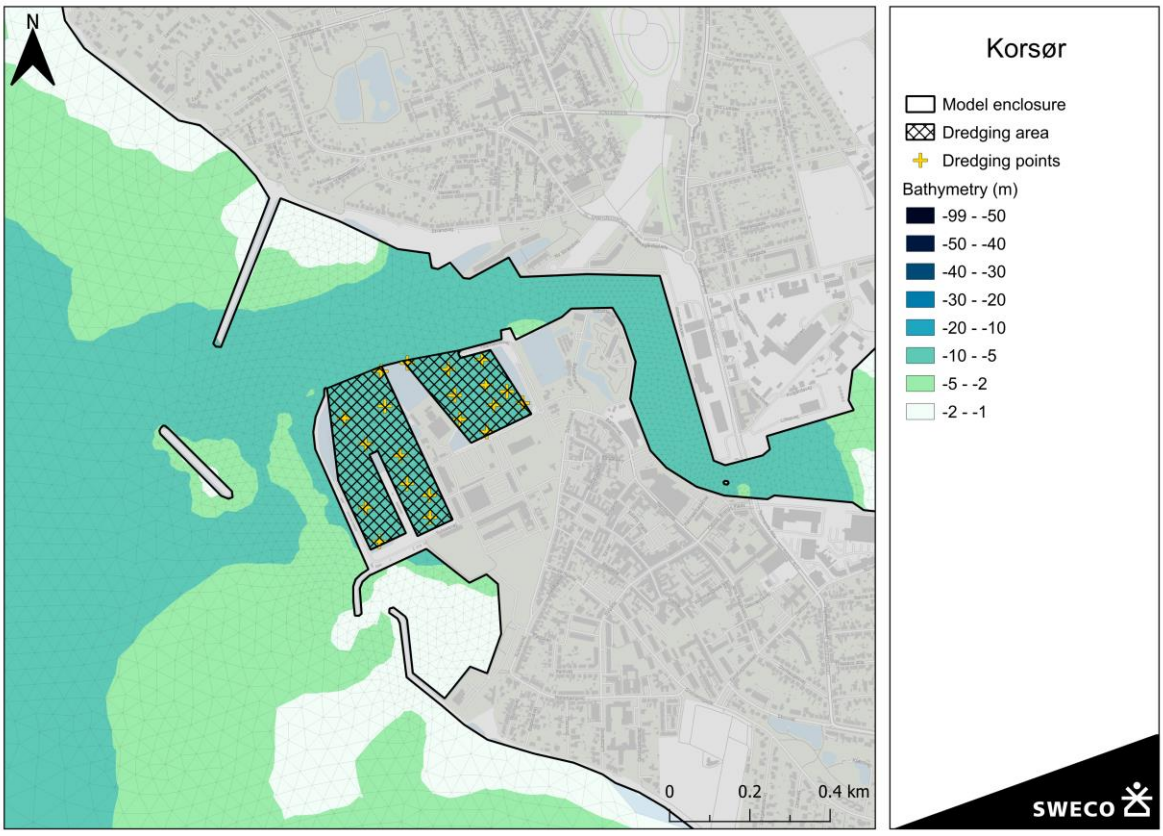

Figure 3.3: Location of the 12 representative dredging points where sediment spill is introduced in the model for a period of 5 days.

Spill of fine sediment can occur at different stages of the dredging. For a grab dredger this occurs at both the grabbing of sediment at the bed, the lifting of the sediment in the bucket, and during the deposition of the sediment in the barge. Based on empirical studies, the total spill that occurs for grab dredging is

estimated between 0 and 5% (WAMSI, 2020), and is assumed conservatively at 5% in the model. This spill is distributed equally over the entire water column. The resulting spill flux is 1.7 kg/s (Table 3.1).

Table 3.1: Calculation of the sediment spill flux based on the production rate, the fraction fine sediments, and the spill rate of a grab dredger.

	Rate (kg/s)
Production rate	97
Production rate for fine sediments (35%)	34
Sediment spill flux (5%)	1.7

The spill flux is distributed over the fine sediment fractions according to the sediment properties (Table 2.1) and results in the spill per fraction as given in Table 3.2. This table also describes the properties of the sediment fractions in the model.

Table 3.2: Properties of the sediment fractions in the model. Sediment fractions larger than 125 µm are not included in the model.

	Clay and fine silt	Medium silt	Coarse Silt	Fine Sand
Diameter (µm)	< 6.3	6.3 - 20	20 - 63	63 - 125
Representative diameter (µm)	3.1	13	42	94
Settling velocity (mm/s)	0.0088	0.15	1.5	7.9
Spill flux (kg/s)	0.233	0.632	0.570	0.275

A sediment retention barrier (a bubble barrier or silt curtain) will be used during the dredging, which will reduce concentrations of suspended sediment and dissolved substances. The use of a sediment retention barrier is not included in the main results but discussed separately in chapter 6.

3.4 Increased concentrations from the dredging spill

Sediment-bound substances will dissolve in the water during the dredging. Different methods are used to calculate the dissolved fraction for either nutrients or environmentally hazardous substances (*miljøfarlige forurenende stoffer*, MFS).

3.4.1 Increase in concentrations of nutrients

The nutrients (TN and TP) that are bound to the sediment, contain a dissolved fraction that will impact the primary production. Within the TN, these are the fractions of dissolved inorganic nitrogen (DIN) and dissolved organic nitrogen (DON). Together DIN and DON make the total dissolved nitrogen (TDN) fraction. Similarly, dissolved organic phosphor (DIP) and dissolved inorganic phosphor (DOP) make the total dissolved phosphorus (TDP). In a study for Odense Havn, experiments were done to study the decomposition of TN and TP (DHI, 2024), for different sediment types. Gyttja (fine-grained, organic-rich sediment) is one of the dominant sediment types in the Korsor area and has the

highest dissolved fractions in the measurements by DHI. Values have been compared with other research and deemed feasible (Christian Lønborg, 2024).

The majority on the release occurs during the first 24 hour, but measurements show an additional fraction being released over the 70 days following this period, but with a much smaller average rate. The pulse within the first 24h is between 4.8 and 6.5% for TDN and TDP respectively. For the remaining days the values drop to ca. 0.09 - 0.06 % per day. The daily rate after day 2 is low with respect to measured variability in DIN and DIP: at the closest NOVANA stations to the project area the coefficient of variance is between 132-178% for DIN and 92-98% for DIP (Aarhus Universitet, 2025). It is calculated that this natural variability is much bigger than the daily added values from the sediment. Therefore, there is no need to add the rate after day 1 in the model calculations. The dissolved fraction is given in Table 2.2.

The release of DIN and DIP is calculated from this data, by combining with the sediment spill rate. Table 3.3 gives the rates and total load in DIN and DIP.

Table 3.3: Release rate and DIN and DIP during dredging. The spill rate is calculated by multiplying sediment spill, with average concentrations (table 2.1) and fraction dissolved (table 1.1). The total load is calculated by multiplying over the total dredging duration of 704 hours.

	Spill rate	Total load
Sediment spill	1.7 kg/s	4.3 million kg
DIN	113 mg/s	286 kg
DIP	57 mg/s	144 kg

The model results are presented relative to background concentrations. Background concentrations have been analysed in NOVANA data: a station inside Korsør Nor (Korsør Nor - 96140001) and another outside the Flådestation in the Great Belt (Karrebæksminde Bugt - 96220008). Measurements were averaged per season. As the worst-case scenario, average concentrations for spring are used for further analyses, as this season has higher phytoplankton growth that utilizes nitrogen and phosphorus. If the dredging will be carried out in another season, then background concentrations are higher, resulting in a lower relative increase of DIN/DIP.

Table 3.4: Measured concentrations per season. Green values are used in the visualisation of the maps as the conservative lower bound. In the tables, the distinction is made between reference concentrations in Korsør Nor and outside this lagoon (yellow and green). The coefficient of variance shows the variance within the dataset over all seasons. Based on data for the period 2005 – 2025.

Parameter	Location	Station	Season				
			Winter	Spring	Summer	Autumn	Coefficient of Variance (%)
TN (mg/l)	Karrebæksminde Bugt	96220008	0.349	0.276	0.276	0.292	31%
	Korsør Nor	96140001 (vmpr 44011)	0.542	0.366	0.447	0.333	48%
DIN (mg/l)	Karrebæksminde Bugt	96220008	0.117	0.021	0.013	0.031	132%
	Korsør Nor	96140001 (vmpr 44011)	0.256	0.027	0.009	0.020	178%
TP (mg/l)	Karrebæksminde Bugt	96220008	0.036	0.024	0.027	0.035	91%
	Korsør Nor	96140001 (vmpr 44011)	0.027	0.025	0.026	0.020	106%

DIP (mg/l)	Karrebæksminde Bugt	96220008	0.020	0.005	0.010	0.016	92%
	Korsør Nor	96140001 (vmpr 44011)	0.006	0.003	0.003	0.004	98%

3.4.2 Increase in concentrations of environmentally hazardous substances (MFS)

A fraction of the sediment-bound environmentally hazardous substances (*miljøfarlige forurenende stoffer*, MFS) will dissolve in the water. The distribution coefficient K_d [l/kg] describes the equilibrium state between the sediment-bound concentration (c_s) [mg/kg] and the dissolved sediment concentration (c_v) [µg/l] for a fixed control volume (Miljøministeriet, 2010). For each of the substances this parameter is given in Table 2.3.

$$K_d = \frac{c_s}{c_v}$$

Assuming that the sediment and dissolved concentration are transported similarly, a single grid cel can be taken as a fixed control volume. The dissolved fraction (f_d) can now be calculated based on the concentrations of total suspended sediment (TSS). Only the increase in TSS by the dredging spill is included in the calculations while background TSS is ignored, which is a conservative approach.

$$f_d = \frac{1}{1 + K_d TSS}$$

The concentration in the water can now be calculated by:

$$c_v = TSS \cdot c_s \cdot f_d$$

The model results are presented relative to the EQS (Table 2.3).

4 Model validation

To assess the quality and reliability of the hydrodynamic model results, a validation process was carried out by comparing simulation outputs with field observations. The analysis focused on water levels and current velocities.

The water level validation verifies the model's ability to reproduce the wind setup and tidal variation, while current profiles are used to evaluate the accuracy of simulated flow dynamics across different layers.

Metrics and model performance criteria are described in Appendix B.

4.1 Water level

A comparison between modelled and observed water levels was conducted at 11 water level stations within the model boundaries (Figure 4.1). A summary of statistics for all stations is given in Table 4.1.

Water levels at all stations show *excellent* results in the validation with an average error (bias) of -0.03 m, a correlation performance (Spearman) of 0.87 and a model performance (NSE) of 0.67.

Additional validation is done for the station Korsor that is indicative for representing the flow velocities through the lagoon channel that are most important for the transport of the sediment plume. An indicative period of the water levels at Korsor is shown in Figure 4.2. The model follows both the tidal variation and the wind setup well.

Table 4.1: Statistics at water level stations.

	Bias (m)	Spearman (-)	NSE (-)
Aarhus	-0.03	0.86	0.69
Bagenkop	-0.02	0.82	0.58
Ballen	-0.06	0.87	0.63
Fredericia	-0.04	0.81	0.49
Fynshavn	-0.03	0.82	0.60
Hov	-0.03	0.87	0.71
Juelsminde	-0.02	0.89	0.73
Kalundborg	-0.07	0.88	0.55
Korsor	-0.03	0.92	0.75
Reerso	0.01	0.91	0.79
Rodbyhavns	0.00	0.92	0.87
Average	**-0.03**	**0.87**	**0.67**

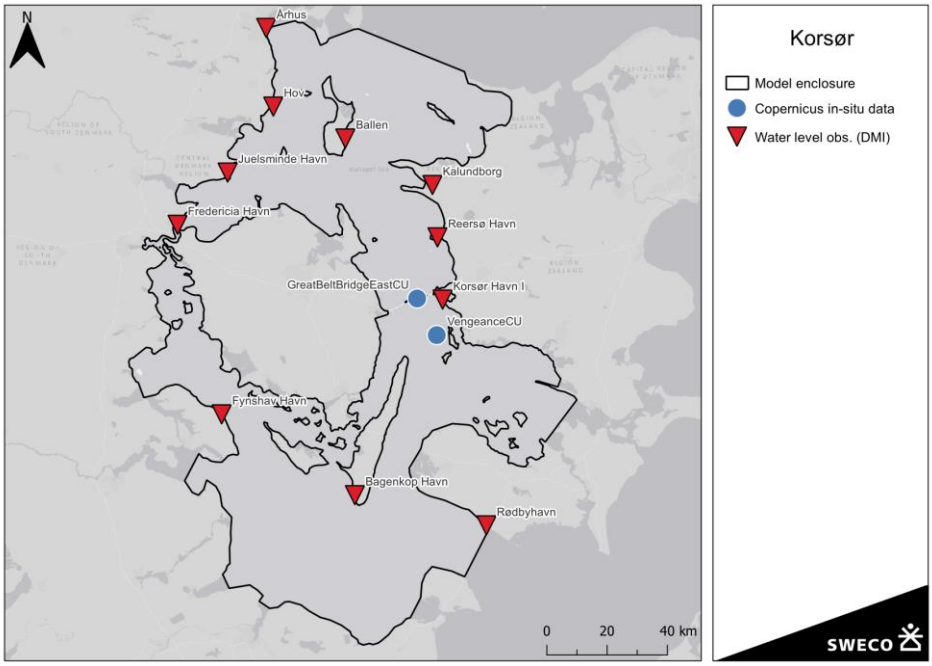

Figure 4.1: Measurement stations used for the validation of the model.

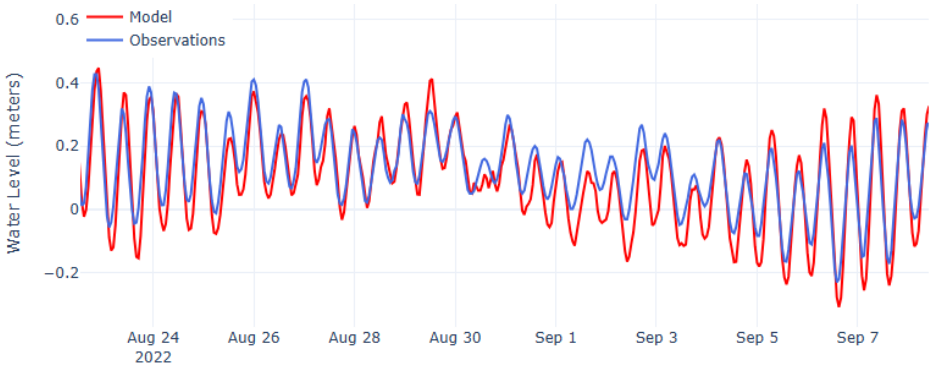

Figure 4.2: Water levels at Korsor between model (red) and measurement (blue).

4.2 Currents

Currents are validated at the stations VengaenceCU and GreatBeltBridgeCU (location shown in Figure 4.1). These are the only available stations with observations of velocity during the model period. The performance indicators for these stations at several depths are shown in Table 4.2. Model results show *very good* correlation (Spearman) between with the observations. However, there is a *poor* result in the (relative) bias: the model results underestimate the flow velocities at both measurements points and at all depths. This also shows in a *poor* result for the model performance (NSE).

An example of the flows at station GreatBeltBridgeCU for a depth of 9 and 3 m, is shown in Figure 4.3. This confirms that the model follows the variation well, but at a lesser magnitude.

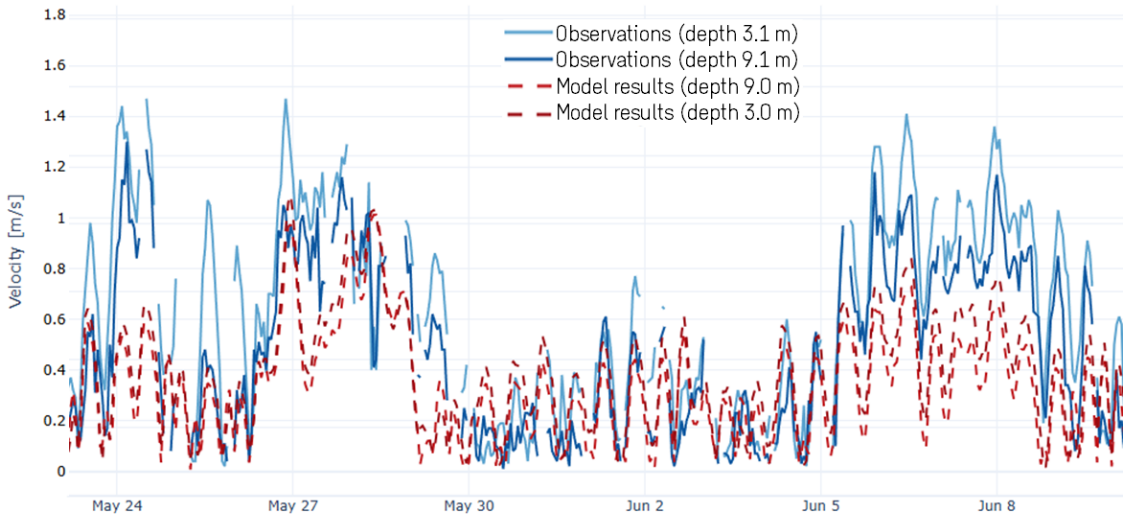

Figure 4.3: Comparison of observed and modelled flow velocity (m/s) at measurement station GreatBeltBridgeCU.

Table 4.2: Comparison on velocity measurements.

	Depth observation (m)	Depth model (m)	Average measured velocity (m/s)	Average modelled velocity (m/s)	Bias (m/s)	Relative bias (%)	Spearman (-)	NSE (-)
VengaenceCU	**1.7**	**1.5**	0.47	0.27	-0.2	-42.6	0.6	0.0
VengaenceCU	**2.7**	**3**	0.47	0.26	-0.2	-42.8	0.6	0.1
VengaenceCU	**5.7**	**6**	0.40	0.24	-0.2	-38.4	0.6	0.2
VengaenceCU	**7.7**	**7.5**	0.35	0.24	-0.1	-31.2	0.7	0.3
VengaenceCU	**8.7**	**9**	0.33	0.23	-0.1	-26.7	0.7	0.3
VengaenceCU	**10.7**	**11**	0.26	0.22	0.0	-8.4	0.6	0.4
GreatBeltBridgeCU	**2.1**	**1.5**	0.60	0.38	-0.2	-39.3	0.7	0.0
GreatBeltBridgeCU	**3.1**	**3**	0.59	0.37	-0.3	-40.7	0.7	0.0
GreatBeltBridgeCU	**6.1**	**6**	0.56	0.34	-0.2	-41.5	0.7	0.0
GreatBeltBridgeCU	**7.1**	**7.5**	0.53	0.32	-0.2	-41.5	0.7	0.0
GreatBeltBridgeCU	**9.1**	**9**	0.44	0.31	-0.1	-29.8	0.6	0.3

4.3 Discharge Lagoon channel

The velocities in the Korsor channel are forced by water level variations in the Great Belt. It can be assumed that water levels in the lagoon Korsor Nor directly follow the water levels at the Great Belt. In the case of a narrow passage (and high flow velocities), tidal choking may occur, introducing a phase lag and tidal attenuation on the inland site of the channel. This is not expected to happen with the limited flow velocities that come from the analysis below.

The discharge Q through the lagoon channel can be calculated using the following equation.

$$Q = \frac{\partial h}{\partial t} \cdot A_{s,lagoon}$$

Where dh/dt is the water level change in the Great Belt at station Korsor and $A_{s,lagoon}$ is the surface area of the lagoon that rises with the tide.

The cross-sectional average velocity can then be calculated by dividing this over the cross-sectional area (A_c)

$$u = \frac{Q}{A_c}$$

The surface area of the lagoon is approximately $8.5 \cdot 10^6$ m^2. The cross section of the lagoon channel is at the smallest 80 m, with a depth of 7 m. Giving an approximate cross-sectional area of 560 m^2.

A comparison of the analytical estimate with the model results in a point at the narrow lagoon channel cross-section, shows good correspondence. The model results are thus plausible.

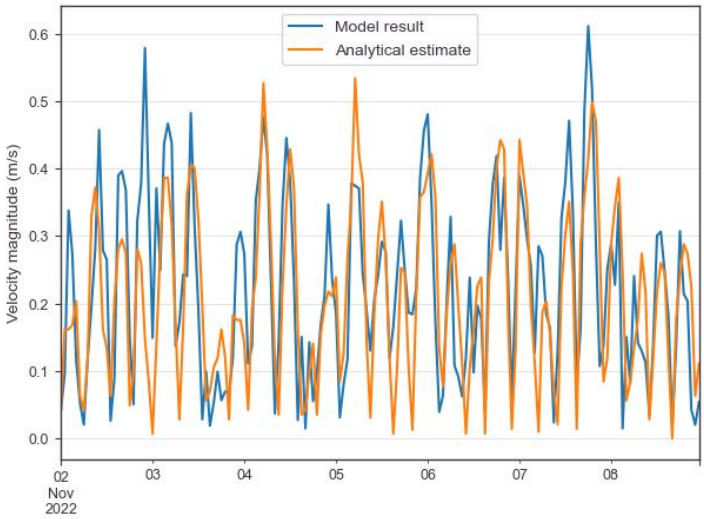

Figure 4.4: Velocity magnitude in the discharge channel.

4.4 Conclusions

The model is found applicable for the study of a sediment plume from dredging at the Korsor port. The currents in the area around the port are dominated by the water level variations on the Great Belt, which have an *excellent* representation in the model. These water level variations stir currents through the lagoon channel. This is captured well by the model when validating with expected velocities through the lagoon channel.

In the Great Belt, the currents are modelled with *very good* correlation, but with a *poor* bias: the currents are much lower than expected from observations. For the dispersion of sediment, low velocities result in the highest concentrations. Low velocities in the Great Belt can thus be considered to give a conservative model result.

5 Model results

This chapter presents the model results on the increase in suspended sediment, the increase in sediment depositions, and the increase in concentrations of nutrients and MFS. These model results do not include the use of a sediment retention barrier.

5.1 Suspended sediment

5.1.1 Indicative results

Spill of sediment during the dredging leads to elevated concentrations of the total suspended sediment (TSS). This results in a sediment plume from the dredging operation that through advective and diffusive processes is transferred over a considerable distance. Settling of the sediment and dilution over larger quantities of water finally reduce the TSS to levels below observable limits.

The Korsor port is located next to a channel leading to the lagoon Korsor Nor. The flow through this lagoon channel is forced most dominantly by the fluctuations in water level at the seaside of this channel. During rising water levels (flood), there is a tidal flow in the channel towards the east, while during falling water levels (ebb) the flow is towards the west.

This tidal variation can also be seen in the modelled sediment plume (TSS). A map (Figure 5.1) and cross section (Figure 5.2) show indicative results of the flows during both flood and ebb. During flood, the sediment plume reaches far into the lagoon. During ebb, the flows into the Great Belt quickly result in large dilution and therefor low TSS concentrations.

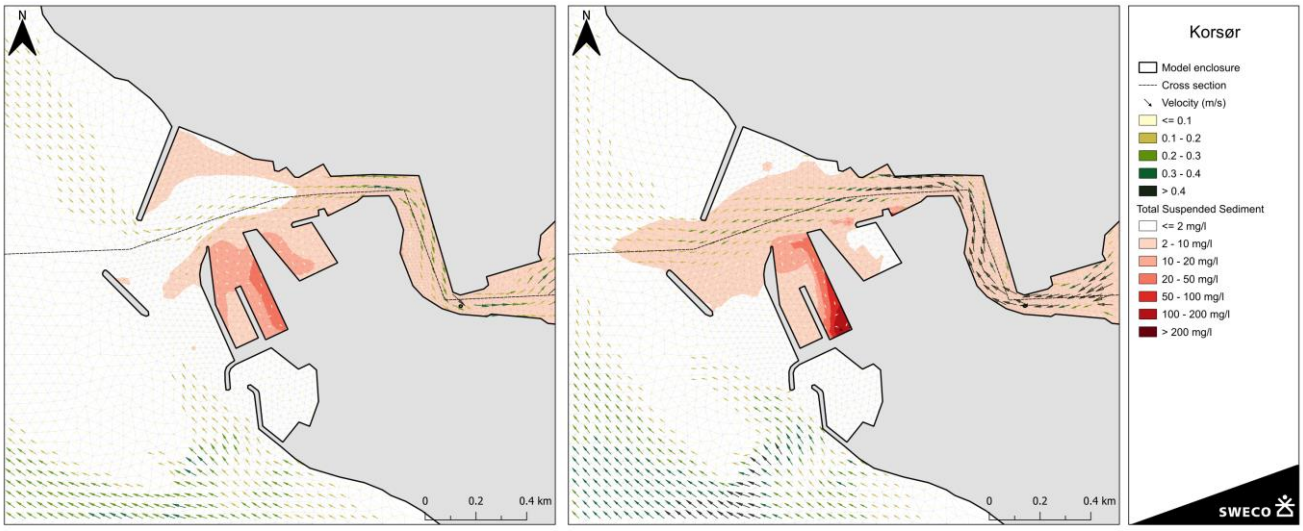

Figure 5.1: Map of the TSS concentration during indicative time steps of flood (left) and ebb (right).

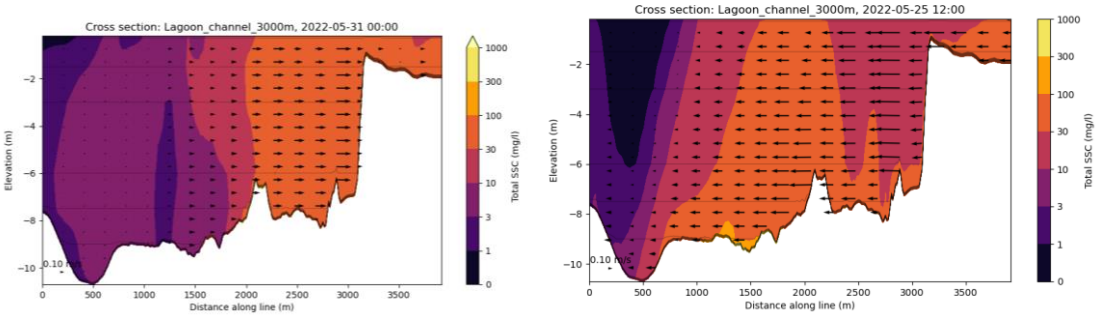

Figure 5.2 Cross section of the TSS concentrations in the channel during indicative time steps of flood (left) and ebb (right). The location of the cross section is shown in Figure 5.1. The entrance to both port basins is located between 1500 and 1800 m.

5.1.2 Statistical maps

The results are summarised in statistical maps. It is noted that all model results exclude background concentrations and only show the increase in TSS concentrations from the dredging.

Figure 5.3 shows average concentration during the 59 days dredging period at both the water surface and bed.

- Average TSS concentrations at the surface do not exceed 5 mg/l. Concentrations up to 2 mg/l reach 250 m west of the port. Average concentrations in the lagoon are between 2 and 3 mg/l.
- Average TSS concentrations at the bed do not exceed 20 mg/l outside of the port basins. Concentrations up to 20 mg/l occur in most of the lagoon channel. Concentrations up to 2 mg/l reach 500 m west of the port. Average concentrations in the lagoon are between 3 and 5 mg/l.

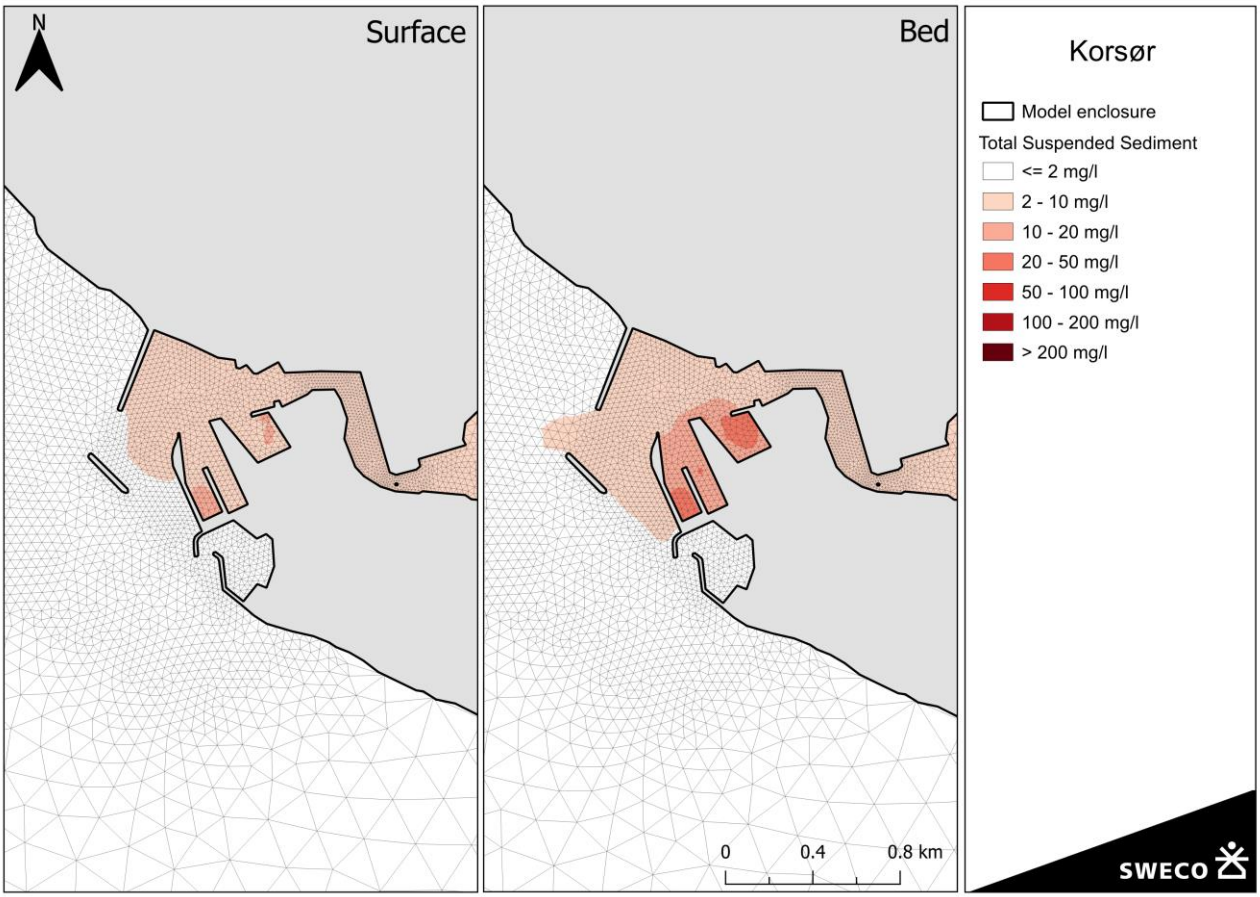

Figure 5.3: Average TSS at surface (left) and bed (right) during the dredging period.

Figure 5.4 shows the maximum concentrations over the entire model period. The maximum map is a compound map where maximum concentrations at one location (one grid cell) do not necessarily occur at the same time as maximum concentrations elsewhere.

- Maximum TSS concentrations at the surface exceed 20 mg/l up to 100 m outside of the port basins. Concentrations up to 2 mg/l reach 2000 m west of the port. Maximum concentrations in the lagoon are around 10 mg/l.
- Maximum TSS concentrations at the bed exceed 50 mg/l up to 100 m around the port basins. Concentrations up to 2 mg/l reach 2500 m west of the port. Maximum concentrations in the lagoon are around 15 mg/l.

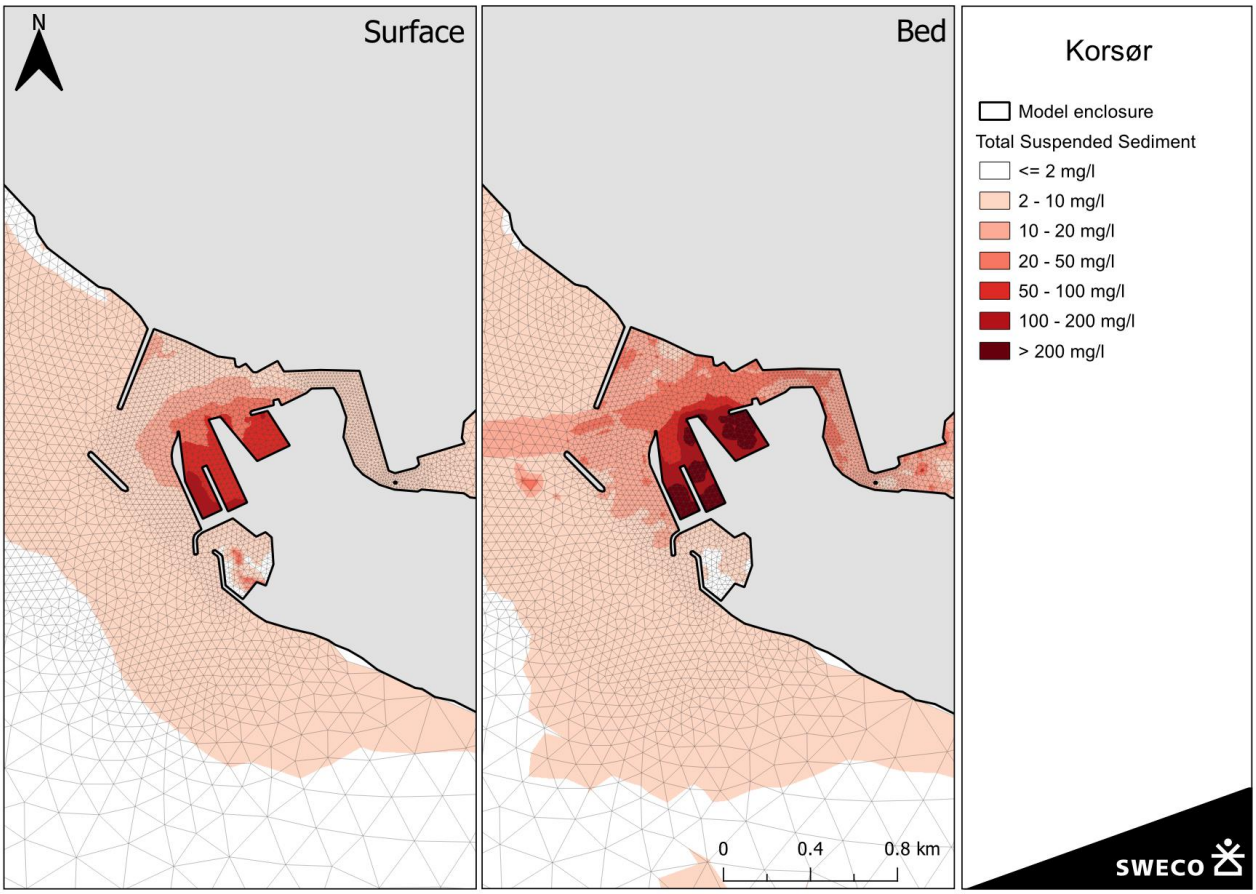

Figure 5.4: Maximum TSS at surface (left) and bed (right).

The duration that depth-averaged TSS concentrations are exceeded is shown in Figure 5.5. This is also a compound map, where for each location (grid cell) the duration can consist of one long period, or many shorter periods, and does not necessarily occur at same time as elsewhere.

- Concentrations of 2 mg/l are exceeded over 12 hours at distances up to 2000 m, and a period of 2 days (48 hours) up to 1500 m. In the lagoon and lagoon channel this concentration is exceeded circa 50 days.
- Concentrations of 5 mg/l are exceeded over 12 hours at distances up to 1000 m, and a period of 2 days (48 hours) up to 600 m. In the lagoon this concentration is exceeded between circa 3 days, but this duration increases to 20 days near the bridge to the lagoon channel. In the lagoon channel this concentration is exceeded circa 25 days.
- Concentrations of 10 mg/l are exceeded over 12 hours at distances up to 400 m, and a period of 2 days (48 hours) up to 150 m. In the lagoon this threshold is exceed less than 12 hours. In the lagoon channel this concentration is exceeded circa 4 days.
- Concentrations of 100 mg/l are not exceeded outside of the port basins.

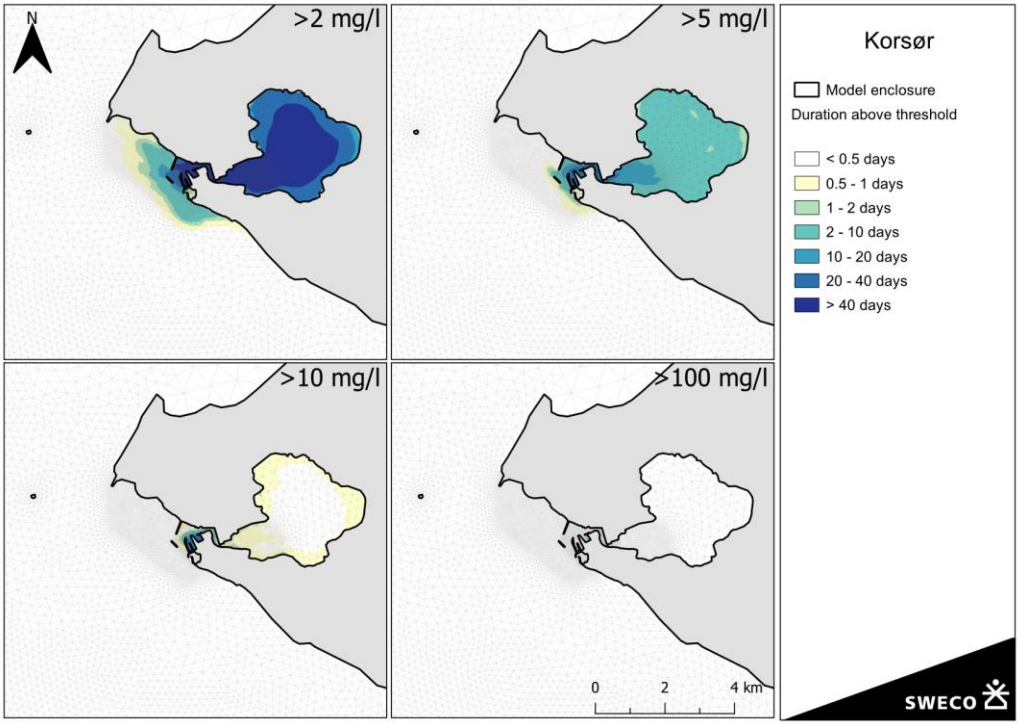

Figure 5.5: Durations of depth-averaged concentrations above given thresholds

5.1.3 Time series

This section presents timeseries of the TSS concentrations at 4 analyses points (Figure 5.6). In Figure 5.7 the variation over the depth is shown but only for a period of 7 days. In Figure 5.8 the entire model period is shown with depth-averaged concentrations.

- The depth variation in Figure 5.7 show that concentrations are usually highest at the bed, but also that the depth variation is relatively limited. The variation over time shows a clear dependency over the tidal cycle for points west of the dredging area (point “Port Entrance”). For these points the concentrations are highest during ebb tide.
- Time series of the depth-average TSS concentrations in Figure 5.8 show the large variation between the hourly and daily data. This is both the result of the dredging cycle (12 hours dredging – 12 hours non-dredging) and the tidal cycle. The exceedance plot supports the results from the earlier analyses of the duration maps in Figure 5.5.

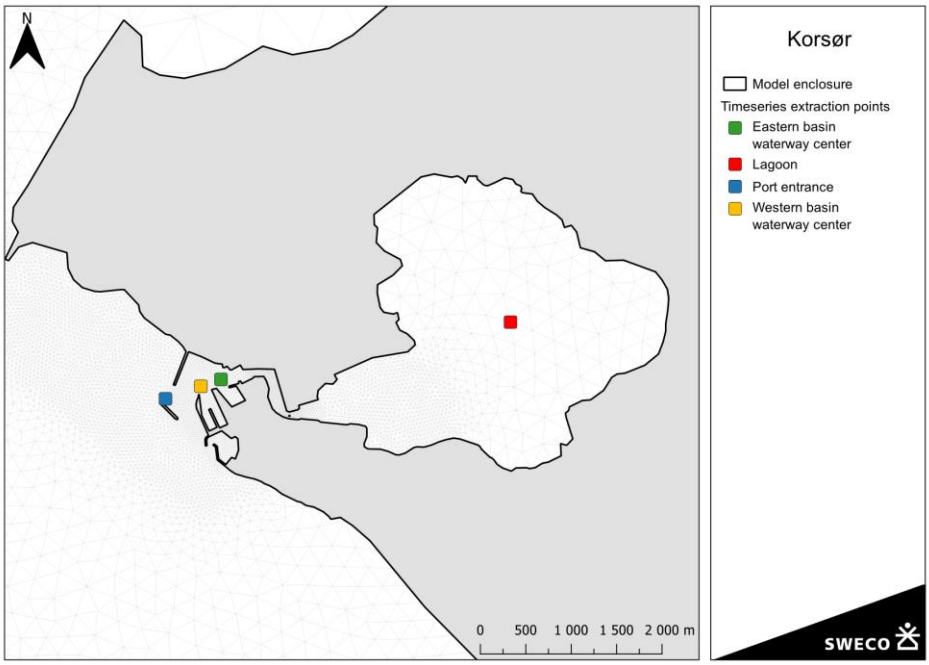

Figure 5.6: Location of timeseries extraction points.

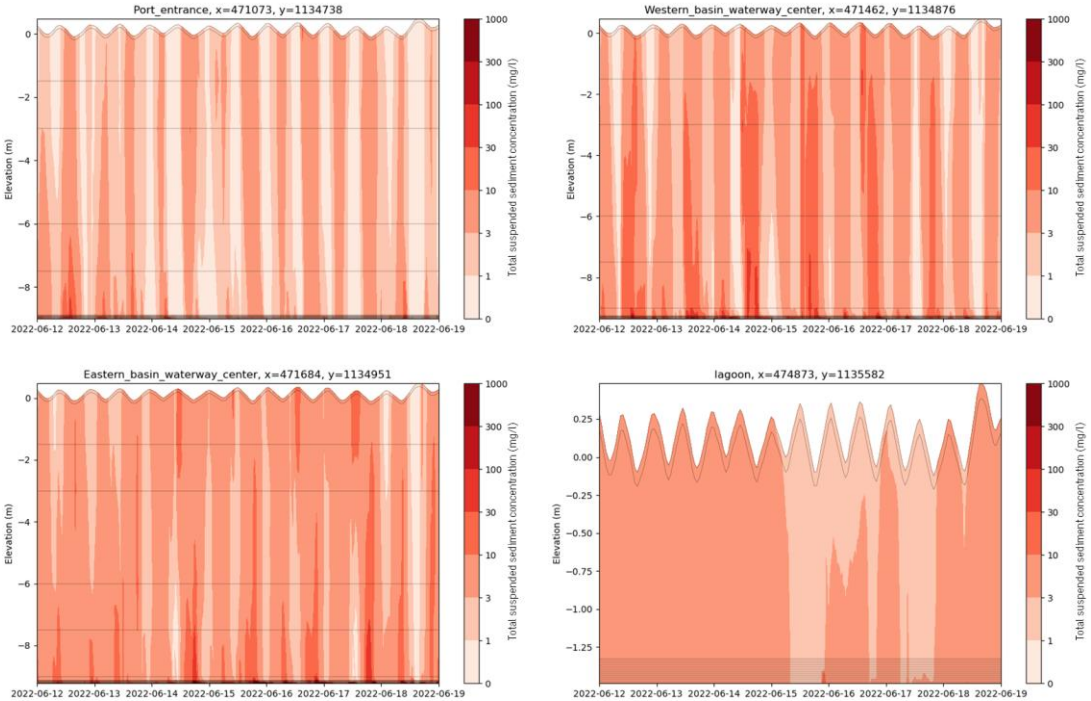

Figure 5.7: TSS concentration with variation over the depth for a period of 7 days. The location of the timeseries extraction points is shown in Figure 5.6.

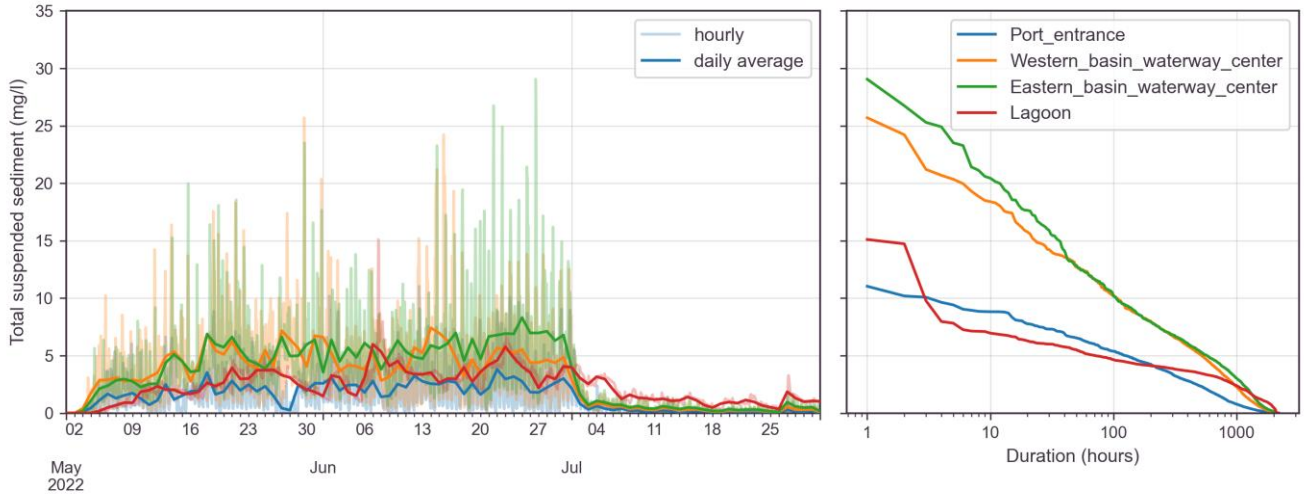

Figure 5.8: Timeseries and exceedance plots of the depth-averaged TSS at 4 analyses points. The location of the timeseries extraction points is shown in Figure 5.6.

5.2 Sediment depositions

The increased TSS concentrations result in an increase in sediment depositions. These depositions can return into suspension when flow velocities exceed the critical shear stresses for the pickup of these (often fine) sediments. A map of the sedimentation at the end of the model run is shown in Figure 5.9.

- The highest deposition is expected within the port basins, where the dredging takes place. Due to the low currents within the port basins, most of the fine sediments sink to the bottom shortly after spilling (63% of total sediment spill). This is most significant for the fractions *Coarse Silt* and *Fine Sand*, which have almost no sediment depositions outside of the port basins.
- In the lagoon, TSS concentrations were shown to be high continuously during the model run. Nevertheless, the sediment depositions are limited and on average only 0,01 mm in the lagoon. The model calculates deposition in few deeper areas where the water depth exceeds 2 m. In other sections of the lagoon, the low water depth results in relatively high flow velocities, continuously bringing the fine sediment fractions back into suspension. Large sections of the lagoon become dry during lower tides. The complicated interaction of these tidal flats with resuspension processes requires additional physical processes that are not included in the model, limiting the accuracy of model results.
- In the lagoon channel, sediment can deposit during tidal slack (between ebb and flood) but will be brought in suspension during the next tidal cycle. At the northern shore, just opposite of the Korsor port, sediment depositions build up during the dredging period and are again resuspended during storm events. At the end of the simulation there is no deposition left.
- Outside of these areas, the sedimentation is limited and never exceeds 0.1 mm. Due to the strong current conditions in the Great Belt most of

the fine sediments do not deposit in the vicinity of Korsor, but are diluted over a large geographical area in the Belt.

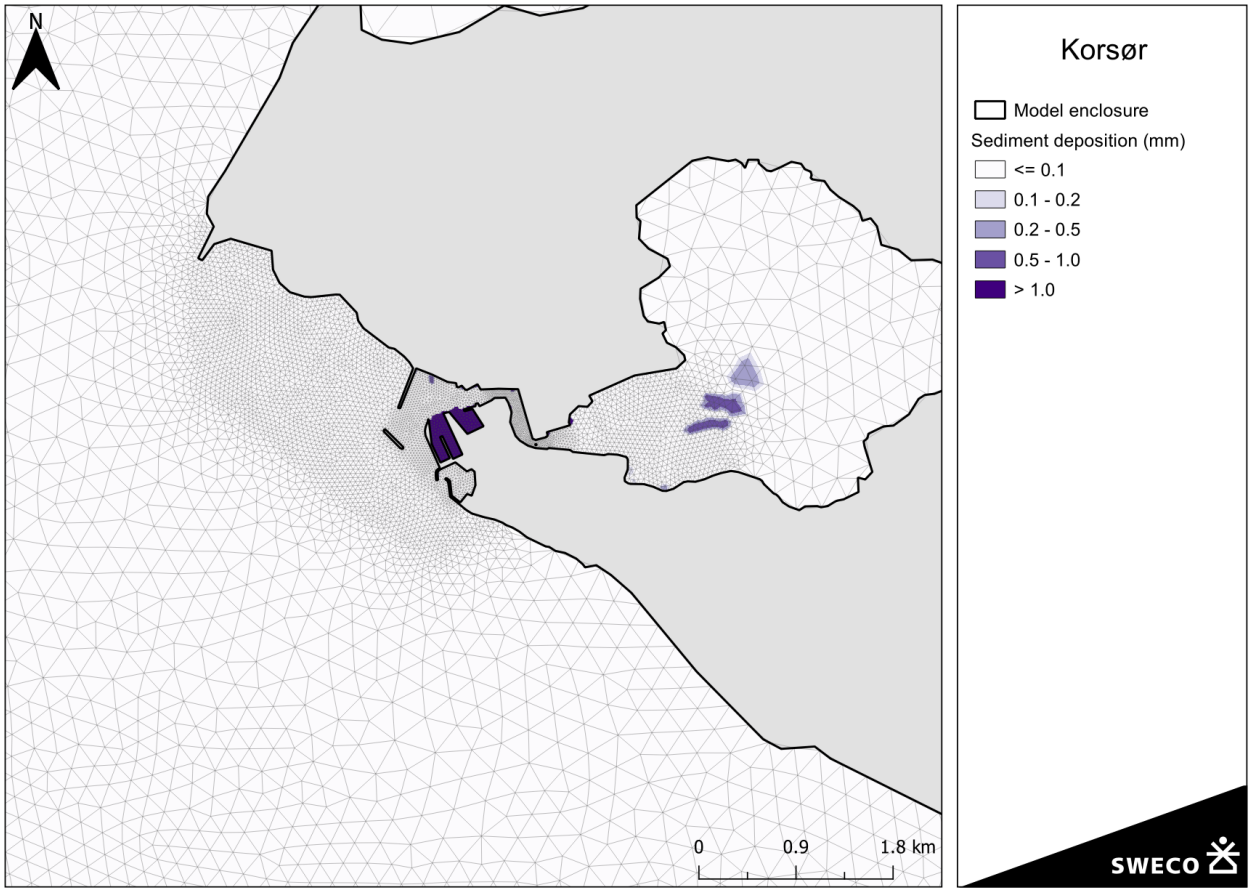

Figure 5.9: Total sediment depositions at the end of simulation

5.3 Increased concentrations

5.3.1 Nutrients

During the dredging, sediment-bound nutrients in the sediment spill are dissolved in the water and cause elevated concentrations of DIN and DIP. Concentrations are calculated following the method in section 3.4.1. The increase concentrations are monitored in three analyses points (Figure 5.10): 2 Novana stations within the lagoon Korsor Nor and an additional point that represents the location in the Great Belt with the highest concentration. Results are presented as timeseries in Figure 5.11 and Figure 5.12.

The results are presented in maps of relative increase in concentrations (Figure 5.13 and Figure 5.14), by dividing the average increased concentration by the measured concentrations during spring. A summary of the results is given in Table 5.1 and Table 5.2.

At station 96140046 in Korsor Nor the increase of DIN is 4.9% and of DIP is 22.2%. In the Great Belt the increase of DIN is 1.0% and of DIP 2.2%.

Figure 5.10: Location of analyses points used in the study of nutrients and MFS.

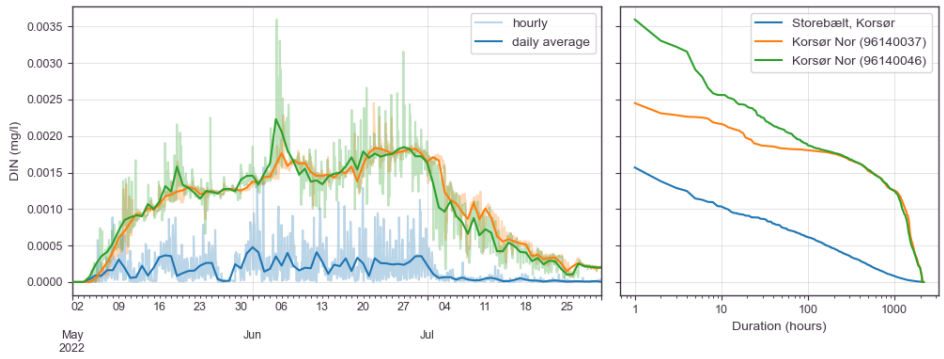

Figure 5.11: Increase in DIN from the dredging activities.

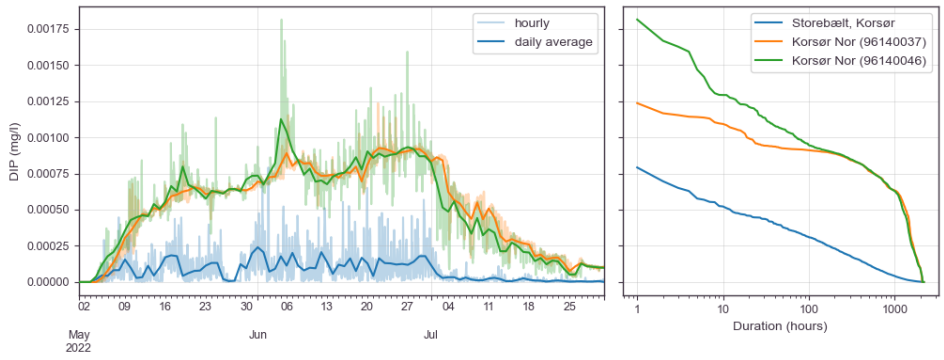

Figure 5.12: Increase in DIP from the dredging activities.

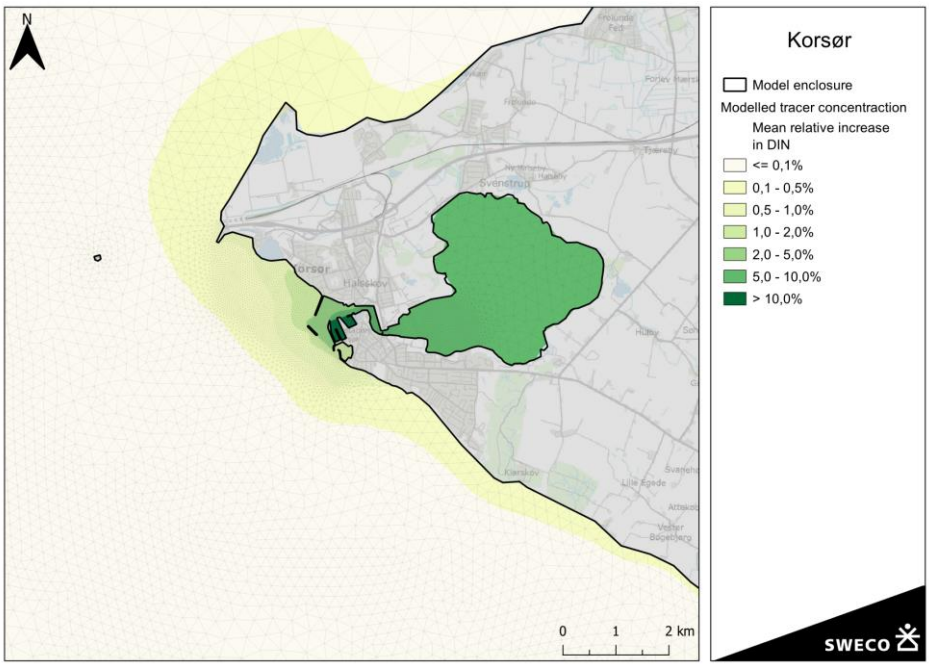

Figure 5.13: Increase in DIN. Average depth-averaged increase during the dredging period. Relative to the measured concentration in spring of 0.021 mg/l.

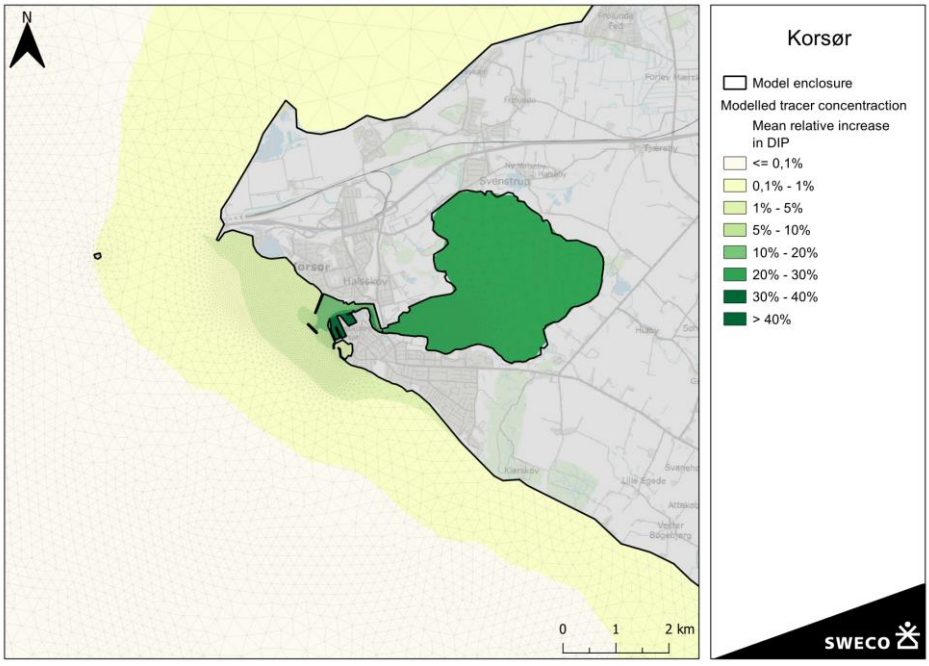

Figure 5.14: Increase in DIN. Average depth-averaged increase during the dredging period. Relative to the measured concentration in spring of 0.003 mg/l.

Table 5.1: Relative increase in DIN

	Background concentration (mg/l)	Mean increase in concentration (mg/l)	Total concentration (mg/l)	Relative increase (%)
Korsør Nor (96140037)	0.027	0.0013	0.028	4.7%
Korsør Nor (96140046)	0.027	0.0013	0.028	4.9%
Storebælt, Korsør	0.021	0.0002	0.021	1.0%

Table 5.2: Relative increase in DIP

	Background concentration (mg/l)	Mean increase in concentration (mg/l)	Total concentration (mg/l)	Relative increase (%)
Korsør Nor (96140037)	0.003	0.0006	0.004	21.4%
Korsør Nor (96140046)	0.003	0.0007	0.004	22.2%
Storebælt, Korsør	0.005	0.0001	0.005	2.2%

Additionally, the results are also expressed as the increased load to the lagoon Korsor Nor in Figure 5.15 and Figure 5.16. This is calculated as the cumulative flow through the lagoon channel. During the dredging period the load DIN to the lagoon increases to 17 kg. For DIP the load goes up to 9 kg. After the dredging period, the tidal currents exchange water between the lagoon and the Great Belt, reducing the increased load to the lagoon. After approximately 1 month the concentrations in the lagoon are back to situation before dredging.

Comparing with the total load in Table 3.3 (286 kg and 144 kg respectively), it can be concluded that less than 10% of the total spill reaches the lagoon Korsor Nor.

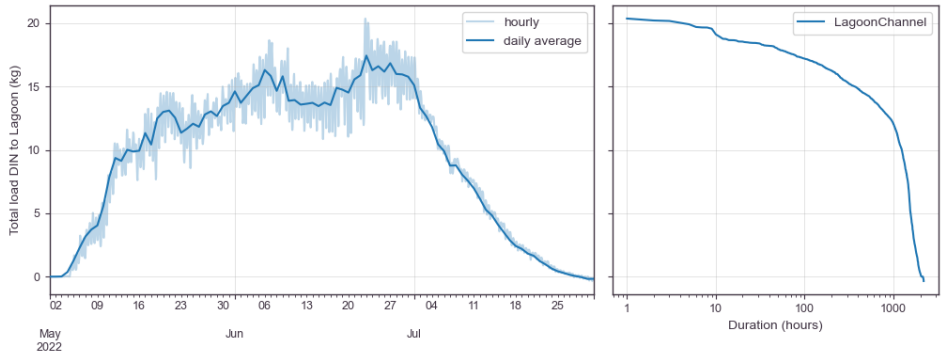

Figure 5.15: Total increased load DIN to the lagoon Korsor Nor by the dredging activities.

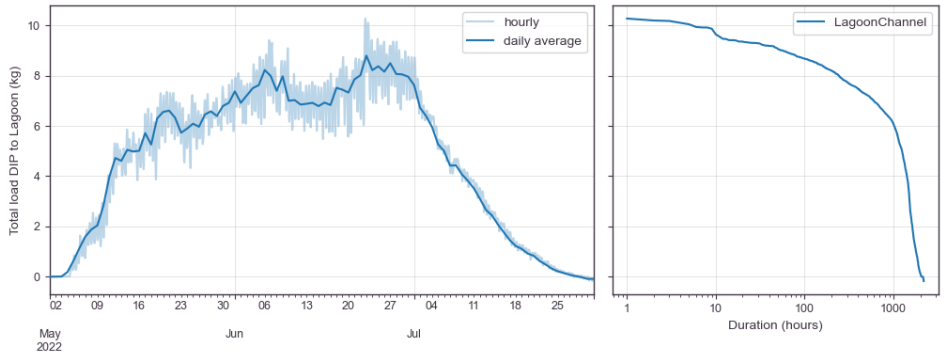

Figure 5.16: Total increased load DIP to the lagoon Korsor Nor by the dredging activities.

5.3.2 Environmentally hazardous substances (MFS)

In Figure 5.8 it was shown that the average TSS concentrations during the dredging period are 4 mg/l in the lagoon Korsor Nor. For this TSS concentration, the dissolved fraction (f_d), the equilibrium concentration (c_w) and the relative increase to the EQS (Δ) are calculated using the method described in section 3.4.2.

Results are given in Table 5.3. The maximum increase are found for Benz(a)pyren, Indeno(1,2,3-cd)pyren and Benz(ghi)perylen at 14% and 15%.

A map of the increase in concentration Benz(a)pyren is given in Figure 5.17.

Table 5.3: Concentration of MFS in the modelled spill, and the maximum concentrations in Korsor Nor. For a TSS concentration of 4 mg/l.

Komponent	National og EU fastsatte miljøkvalitetskrav for vand, EQS [ug/l]	Dissolved fraction [%]	Equilibrium concentration in control volume [ug/l]	Increase, relative to EQS [%]
Tungmetaller				
Arsen, As	2.6	100%	0.022	1%
Bly, Pb	1.3	46%	0.024	2%
Cadmium, Cd	0.2	66%	0.001	0%
Chrom (total), Cr	3.4	67%	0.073	2%
Kobber, Cu	1.2	91%	0.116	10%
Kviksølv, Hg */**	0.07	60%	0.000	0%
Nikkel, Ni	8.6	97%	0.097	1%
Zink, Zn	8	99%	0.294	4%
PAH'er				
Phenanthren	0.94	92%	0.000	0%
Antracen	0.1	90%	0.000	0%
Fluoranthen	0.0063	99%	0.0002	4%
Pyren	0.0023	81%	0.0002	10%
Benz(a)anthracen	0.0005	33%	0.0000	7%
Chrysen	0.0014	28%	0.0000	3%
Benz(a)pyren	0.00017	16%	0.00002	14%
Indeno(1,2,3-cd)pyren	0.00017	16%	0.00002	14%
Benz(ghi)perylen	0.00017	16%	0.00003	15%
Nonylphenoler	0.3	89%	0.000	0%
Methylnaphthalener, mono, di og tri	0.12	98%	0.001	1%
Sum af PFOA, PFOS, PFNA, PFHxS, høj LOD	0.00013	99%	0.00000	3%

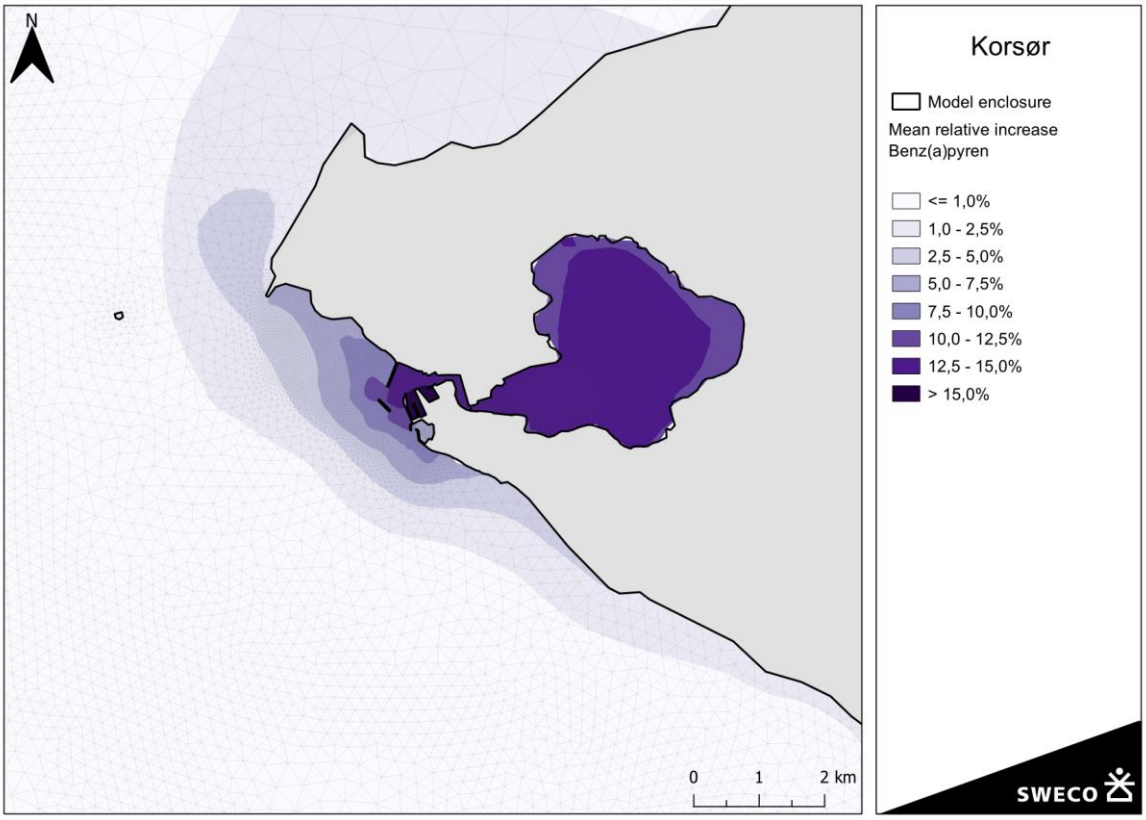

Figure 5.17: Mean increase in concentrations Benz(a)pyren, relative to the EQS.

6 Results when including sediment retention barrier

6.1 The efficiency of bubble curtains

The project will use a double bubble curtain to limit the environmental impact of sound and suspended sediment.

The location of the bubble barrier impacts its effectiveness. Three bubble curtains are planned (Figure 6.1). On the interface of the basin and the lagoon channel (green and blue) the effective is highest due to low flow velocities but collides with the land reclamation. Inside of the lagoon channel (red) the effective is expected lower because of the higher flow velocities from tidal currents.

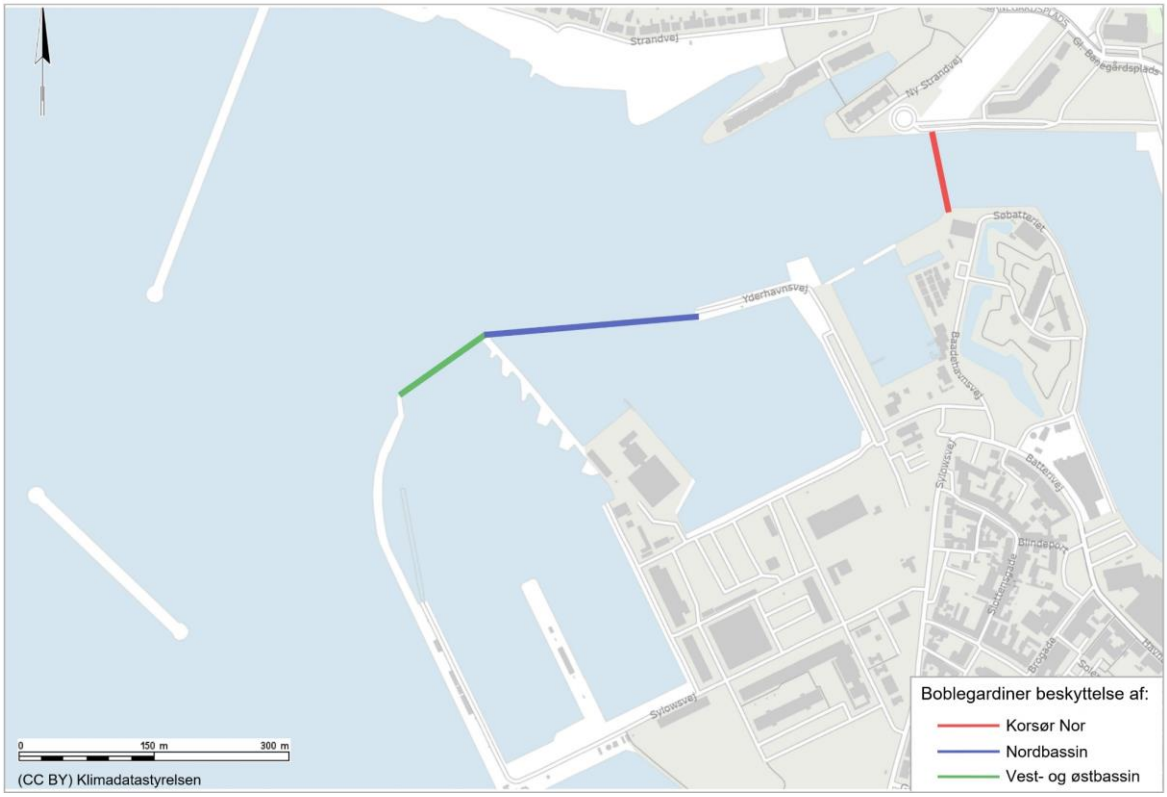

Figure 6.1: Planned placement of three bubble barriers.

Bubble curtains are a frequently used solution and have proven to be effective for the mitigation of sound. Its function as a sediment retention barrier (Figure 6.2) has been less documented, although usage from practise suggests a high efficiency. A selection from available sources:

- PIANC guidelines mention that it has large benefits with the logistics of transport, but that it can only be used under certain conditions. (PIANC, 2009)

- Scale model experiments have been carried out for different sediment fractions in a flume with depth of 24 cm, and flow velocity of 0.2 m/s. Results show that two micro bubble curtains give a reduction in suspended sediment of 78%. Results vary per sediment size but show no clear correlation. (Callaway R, 2018) (Mendzil, 2018)
- Additional scale model experiments (depth up to 80 cm, flow velocity up 0,1 m/s) show that the bubble curtain generates flow circulation cells. As sediment, the experiments use synthetic particles with a diameter of 3.14 mm and density of 1410 kg/m^3. Results of the current-driven experiments show an efficiency in sediment reduction of 95%. (Covarrubias-Contreras, 2025)
- Manufacturers of bubble curtains mention that they work in currents, and up to depths of 35 m. Continuous measurements in the field have supposedly proven its effect. Unfortunately, these results are not openly shared. (WAENS, 2023)

None of these studies share estimates on the efficiency in practise, where higher flow velocities, larger depths, and different types of bubbles impact the efficiency. Due to the uncertainty in the efficiency, the effects of a sediment retention barrier are shown for 3 possible efficiencies: a 25%, 50 and 75% reduction in suspended sediment.

Figure 6.2: Example of the usage of a bubble curtain (PIANC, 2009).

6.2 Effect on sediment concentrations

The sediment concentrations are shown for 3 possible efficiencies of a bubble curtain: 25%, 50% and 75% reduction in suspended sediment. Few representations of the model results are repeated for each of these efficiencies.

Maps of the duration that sediment concentrations exceed either 2 mg/l or 5 mg/l are shown in Figure 6.3 and Figure 6.4 respectively. The reference situation without a bubble curtain is included.

- Exceedance of 2 mg/l (Figure 6.3) occurred over 40 days without a bubble curtain. With a bubble curtain of 25%, 50% and 75%, this reduces to 20 days, 10 days, and less than 1 day respectively.

- Exceedance of 5 mg/l (Figure 6.4) occurred circa 5 days without a bubble curtain. With a bubble curtain of 25%, 50% and 75%, this reduces to 1 days, up to half a day, and never.

Timeseries and duration-exceedance plot of concentrations at four descriptive points are given in Figure 6.5. Results show the expected reduction by 25%, 50% and 75%.

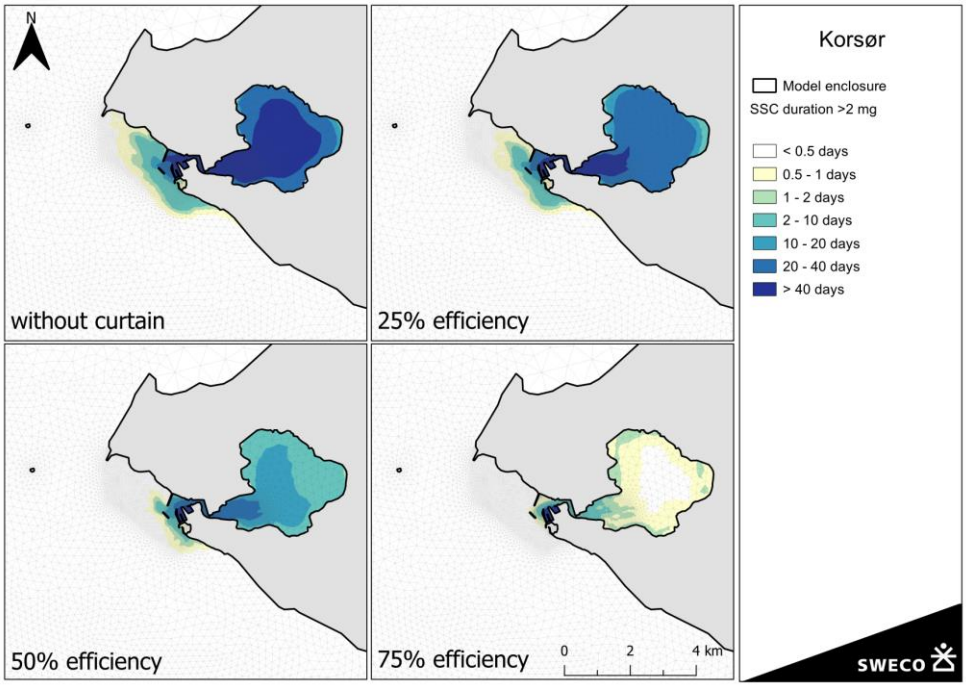

Figure 6.3: Durations of depth-averaged concentrations above 2 mg/l for different efficiencies of a bubble barrier.

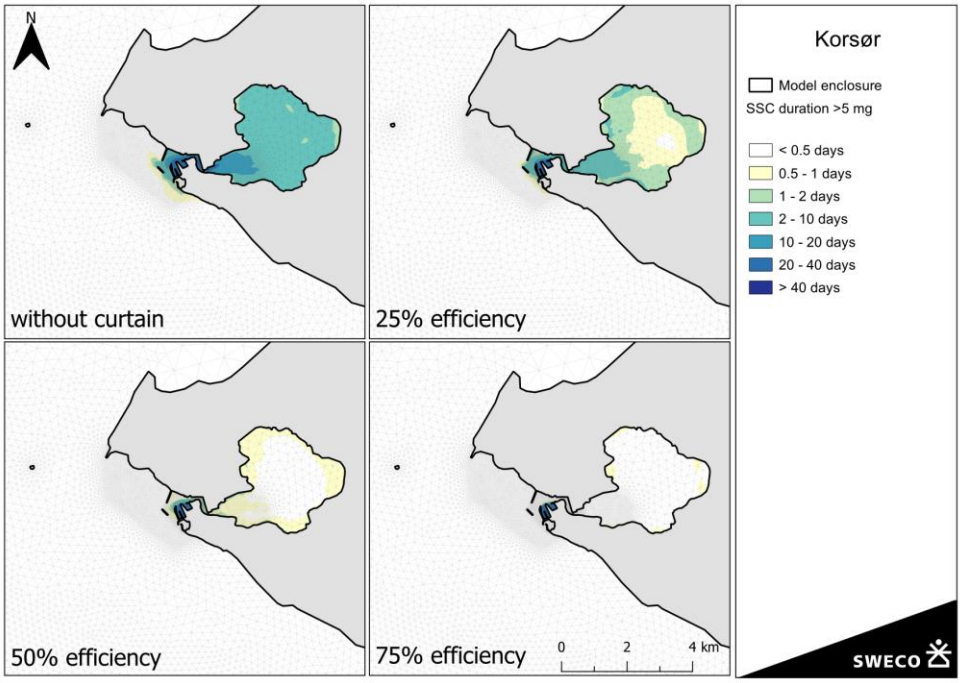

Figure 6.4: Durations of depth-averaged concentrations above 5 mg/l for different efficiencies of a bubble barrier.

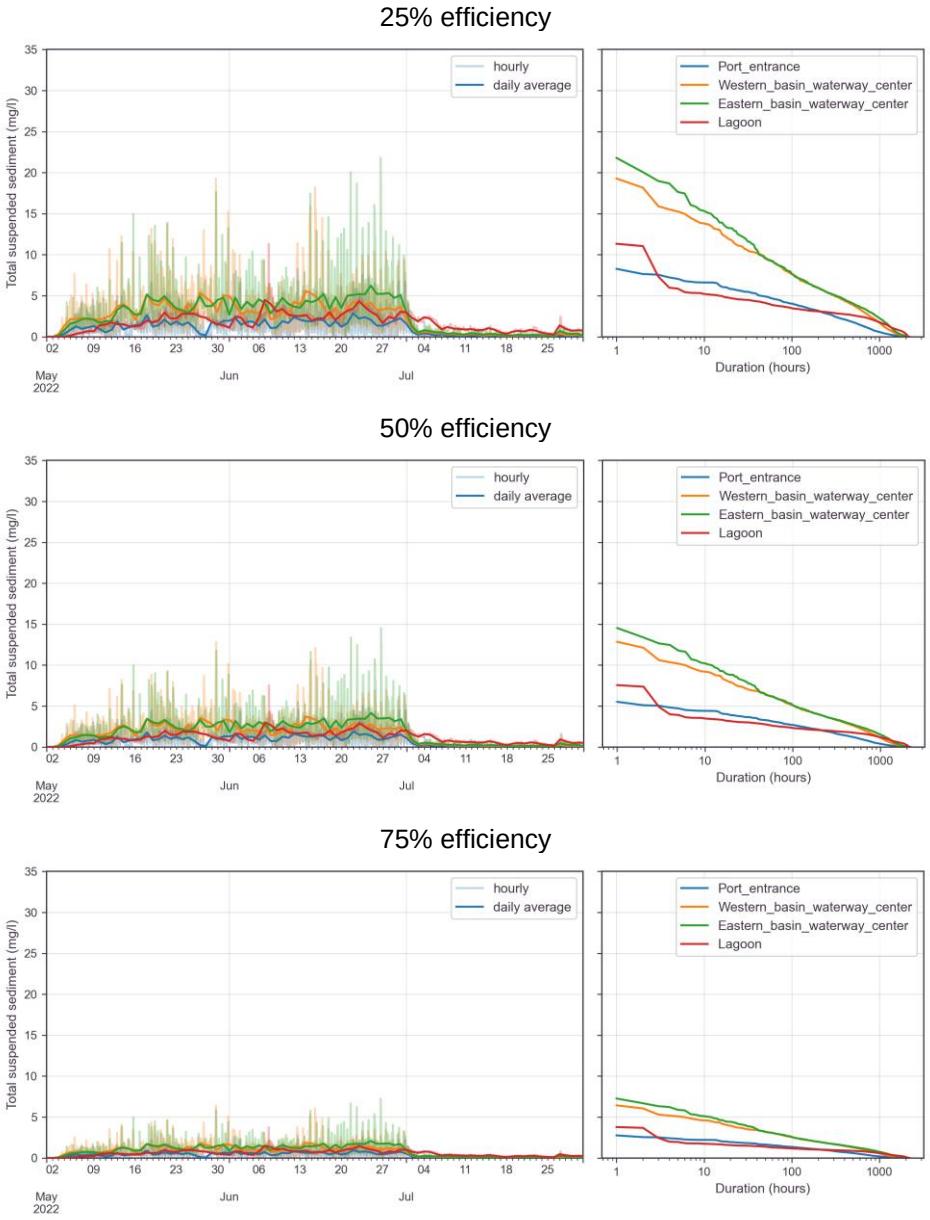

Figure 6.5: Timeseries and exceedance plots of the depth-averaged TSS at 4 analyses points for different efficiencies of a bubble curtain. The results without bubble curtain are shown in Figure 5.8. The location of the timeseries extraction points is shown in Figure 5.6.

6.3 Effect on nutrients

Similar to the sediment concentrations, the effects of a sediment retention barrier are shown for 3 possible efficiencies: a 25%, 50% and 75% reduction in concentrations in Table 6.1 and Table 6.2.

Table 6.1: Relative increase in DIN, including bubble curtain with assumed efficiency.

	without curtain	25%	50%	75%
Korsør Nor (96140037)	4.7%	3.5%	2.4%	1.2%
Korsør Nor (96140046)	4.9%	3.7%	2.4%	1.2%
Storebælt, Korsør	1.0%	0.8%	0.5%	0.3%

Table 6.2: Relative increase in DIP, including bubble curtain with assumed efficiency.

	without curtain	25%	50%	75%
Korsør Nor (96140037)	21.4%	16.0%	10.7%	5.3%
Korsør Nor (96140046)	22.2%	16.7%	11.1%	5.6%
Storebælt, Korsør	2.2%	1.6%	1.1%	0.5%

7 Summary

A 3D hydrodynamic model has been built to study the transport of a sediment plume from the dredging in the Naval Port Korsor. The model covers the entire Great Belt Sea between Aarhus and Rodbyhavn. By choosing a large extend, the model is expected to best calculate the velocities from the barotropic and baroclinic inflows. Model results show excellent results for the water level variations but show a poor model performance for the velocities. As the flow velocities through in the lagoon channel, adjacent to the port basins, are dominantly driven by water level variations, the model is applicable for this study.

Model results show that the increased TSS concentrations from the sediment spill are transported with the tide. During ebb tides, the sediment is transported to the Great Belt, where the high flows quickly dilute to low concentrations. During flood tides, the sediment is transported to the lagoon Korsor Nor. In the lagoon elevated TSS concentrations occur for most of the dredging period. The sediment is however limited, due to the flushing out of sediment depositions at lower water levels.

Concentrations of nutrients and environmentally hazardous substances (MFS) are increased due to the dissolving of the sediment-bound concentrations in the sediment spill. The increased concentrations of these substances shows a very similar spatial and temporal distribution. In Korsor Nor, the increase of DIN is 4.9% and of DIP is 22.2%, relative to the measured concentrations during spring. Of all MFS, the highest increase in concentrations is found for Benz(a)pyren, Indeno(1,2,3-cd)pyren and Benz(ghi)perylen at 14% and 15%, relative to the environmental quality standards. After the dredging period it takes circa a month for the lagoon Korsor Nor to fully recover.

A bubble barrier could be considered as a sediment retention barrier. Model results are presented given assumed efficiency of 25%, 50% and 75% for both sediment concentrations and nutrients.

8 References

Aarhus Universitet. (2025). *Overfladevandsdatabasen*. Hämtat från NOVANA: https://odaforalle.au.dk/login.aspx

Callaway R, D. R. (2018). *Micro bubble curtains: impact on Sediment Dispersal, SEACAMS2 Project (SC2-R&D-SU03).* Swansea University, pp. 19, 2018. .

Christian Lønborg, S. M. (2024). Impacts of anthropogenic resuspension on sediment organic matter: An experimental approach.

Covarrubias-Contreras, B. T.-F. (2025). *Interaction between a bubble curtain with waves and currents: implications on sediment dispersal.* Environ Fluid Mech 25, 14 (2025). https://doi.org/10.1007/s10652-025-10029-1.

DHI. (2019). *Development of Mechanistic models. Assessment of model performance.*

DHI. (2024). *Odense Havn. Ny sejlrende og udvidelse af terminalområdet. Frigivelse af næringsstoffer ved planlagt udvidelse af Odense Havn. 11830790.*

Jakobsen, F. e. (2010). *Flow resistance in the Great Belt, the biggest strait between the North Sea and the Baltic Sea.*

Mendzil. (2018). *Micro bubble curtains: impact on Sediment Dispersal Supplementary Report. SEACAMS2 Project (SC2-R&D-SU03) .*

Miljøministeriet. (2003). *Genbesøget af vandområdeplaner 2021-2027: Udkast til bekendtgørelse om fastlæggelse af miljømål for vandløb, søer, overgangsvande, kystvande og grundvand.*

Miljøministeriet. (2010). Kemiske stoffer. Vurdering af stoffer i forhold til farlighed i grundvandet.

Miljøstyrelsen. (2025, 10 23). *Kvalitetskriterier for miljøfarlige forurenende stoffer i vandmiljøet*. Retrieved from https://mst.dk/erhverv/sikker-kemi/kemikalier/graensevaerdier-og-kvalitetskriterier/kvalitetskriterier-for-miljoefarlige-forurenende-stoffer-i-vandmiljoeet

PIANC. (2009). *Dredging Management Practices for the environment. A structured selection approach. Report 100 - 2009 (EnviCom).*

Sweco. (2025). Extension of the Naval station Korsor. Hydrodynamic model simulation of the sediment spill from dredging (internal draft, 2025-06-06).

WAENS. (2023). *Information om bubbelgardiner.*

WAMSI. (2020). *Guideline on dredge plume modelling for environmental impact assessment.*

Appendix A: Data availability

	Station ID	Station name	Period	Variables	Depth range	Time interval	Source	Measured by
1	NO_TS_MO_1000044	Kiel Lighthouse	1985-06-20 - 2025-01-31	Salinity, sea temp	19	Hourly	Copernicus Marine In Situ	BSH
2	NO_TS_MO_6600023	Fehmarn Belt Buoy	1990-01-02 – 2024-02-29	Current speed, current dir, salinity, sea temp	27	Hourly	Copernicus Marine in Situ	BSH
3	BO_PR_CT_SMHI925KATTEGATSW	925 KATTEGAT SW	1991-06-16 – 2023-01-11	Salinity, sea temp	50	Irregular (yearly?)	Copernicus Marine in Situ	
4	BO_TS_MO_SpodsbjergLtCU	Spodsbjerg Lt CU	2024-11-25 - 2025-02-01	Current speed, current dir, salinity, sea temp	26		Copernicus Marine in Situ, SMHI	FCOO
5	BO_TS_MO_HatterBarnCU	Hatter Barn CU	2023-05-17 - 2025-04-01	Current speed, current dir	14		Copernicus Marine in Situ, SMHI	FCOO
6	BO_TS_MO_GreatBeltBridgeEastCU	Great Belt Bridge East CU	2022-05-01 - 2025-04-01	Current speed, current dir	13		Copernicus Marine in Situ, SMHI	FCOO
7	BO_TS_MO_VengeanceCU	Vengeance CU	2007-03-27 - 2025-04-01	Current speed, current dir	13		Copernicus Marine in Situ, SMHI	FCOO
8	94010051	Syd for Hjelm dyb	2010-07-07 - 2024-11-20	Salinity, sea temp	50		DCE***	
9	94300001	Nordlige Lillebælt	2010-01-12 - 2024-12-12	Salinity, sea temp	20		DCE	
10	94300013	Mejl Flak Vest	2010-01-26 - 2024-12-05	Salinity, sea temp	18		DCE	
11	95200004	6100051	2010-07-06 - 2024-11-29	Salinity, sea temp	45		DCE	
12	95300001	6100021	2010-01-13 - 2024-12-12	Salinity, sea temp	34		DCE	
13	95600010	7301801	2010-07-08 - 2024-12-10	Salinity, sea temp	35		DCE	
14	96100015	6700053	2010-01-11 - 2024-12-05	Salinity, sea temp	36		DCE	
15	96100041	DMU station 939	2010-09-24 - 2024-10-24	Salinity, sea temp	38		DCE	
16	96100042	DMU station 935	2010-09-24 - 2024-10-18	Salinity, sea temp	52		DCE	
17	96140001	vmpr 44011	2010-04-08 - 2024-12-19	Salinity, sea temp	2,7		DCE	
18	96400034	7701506	2018-08-14 - 2024-11-26	Salinity, sea temp	45		DCE	

19	96400041	DMU station 443	2010-09-23 - 024-11-26	Salinity, sea temp	37		DCE	
20	98100008	7301702	2010-07-08 - 2024-11-26	Salinity, sea temp	32		DCE	
21		Aarhus	Since 1995	Water level			DMI	DMI
22		Ballen Havn	Since 2012	Water level			DMI	DMI
23		Fredericia	Since 1995	Water evel			DMI	DMI
24		Fynshavn	Since 1995	Water level			DMI	DMI
25		Gedser	Since 1995	Water level			DMI	DMI
26		Havenbyen	Since 2012	Water level			DMI	DMI
27		Hornbaek	Since 1995	Water level			DMI	DMI
28		Hou	Since 2011	Water level			DMI	DMI
29		Korsor	Since 1995	Water level			DMI	DMI
30		Rodbyhavns	Since 1995	Water level			DMI	DMI

BSH: Das Bundesamt für Seeschifffahrt und Hydrographie

FCOO: Forsvarets Center for Operativ Oceanografi

DCE: Nationalt Center for Miljø og Energi

Appendix B: Goodness of Fit

Goodness of fit can be expressed by many different model parameters. In this study we use the following metrics, which align with similar studies (DHI, 2019):

- The average error is evaluated using either **Bias** or **Percent Bias (P-Bias)**. The P-Bias is preferred, as this is a normalised error value where 0 is a perfect match and any deviation is indicated as a percentage to the average observed value. However, this cannot be used for all parameters, for example for water levels which average around m AD.

$$bias = \frac{1}{n}\sum_{i=1}^{n}(model_i - obs_i)$$

$$P_{bias} = \frac{\sum_1^N (P_i - O_i)}{\sum_1^N O_i} * 100$$

- The correlation is evaluated using the **Spearman Rank Correlation**. This is a variation to the Pearson correlation where both measurements and model results given a rank, and only the difference in rank is evaluated. Compared to the Pearson correlation it is not influenced by the timing. A value of 1.0 mean that the model results are identical to the measurements (with allowed deviation in timing), and a value of 0.0 means there is no correlation.

$$r_s = 1 - \frac{6\sum_1^N (rg_{Oi} - rg_{Pi})^2}{N(N^2-1)}$$

- For the model performance the **Nash-Sutcliffe model efficient coefficient (NSE)** is used, which is the ratio between the model error and the variability in the data. A perfect model will have a score of 1.0, and a score of 0.0 means that the squared error of the model results is identical to the variation in the observations.

$$\mathrm{NSE} = 1 - \frac{\sum_{t=1}^{T}\left(Q_o^t - Q_m^t\right)^2}{\sum_{t=1}^{T}\left(Q_o^t - \overline{Q}_o\right)^2}$$

Table 8.1: Goodness-of-fit metrics. Model performance criteria are taken identical to (DHI, 2019). The error metric Bias has a parameter specific model performance and is specified only for water level as the relative bias is not valid for this error matric.

Goodness-of-fit	Metric	Use for parameters	Model performance			
			Excellent	Very Good	Good	Poor
Bias	Error metric	Water level	< 0,05 m	0,05 – 0,10 m	0,10 – 0,20 m	> 0,40 m
Percent Bias (P-Bias)	Error metric	Salinity, Temperature	< 10%	10 – 20 %	20 – 40%	> 40%
Spearman Rank Correlation	Correlation metric	Water level, Salinity, Temperature	> 0.9	0.9 – 0.6	< 0.6	
Nash-Sutcliffe model efficient coefficient (NSE)	Model performance	Water level, Salinity, Temperature	> 0.65	0.65 – 0.5	0.5 – 0.2	< 0.2

Appendix C: Additional figures on model results

C.1 Suspended sediment

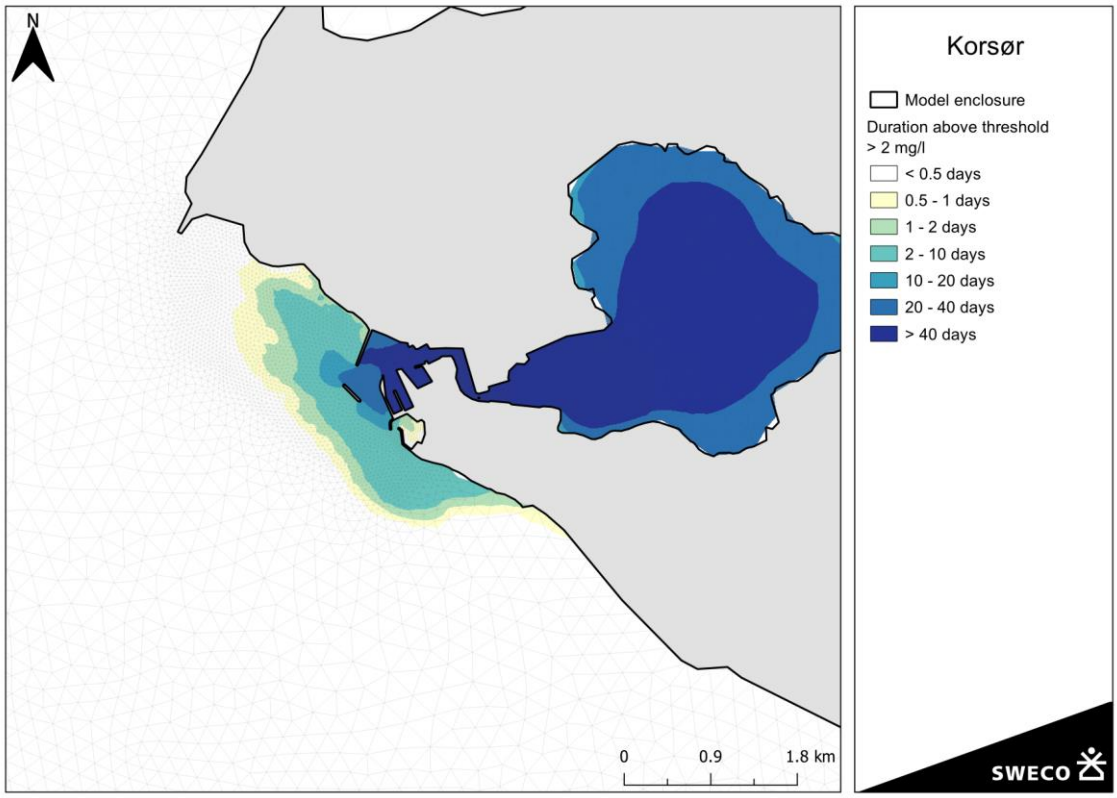

Figure 8.1: Model results without bubble curtain: Duration above 2 mg/l.

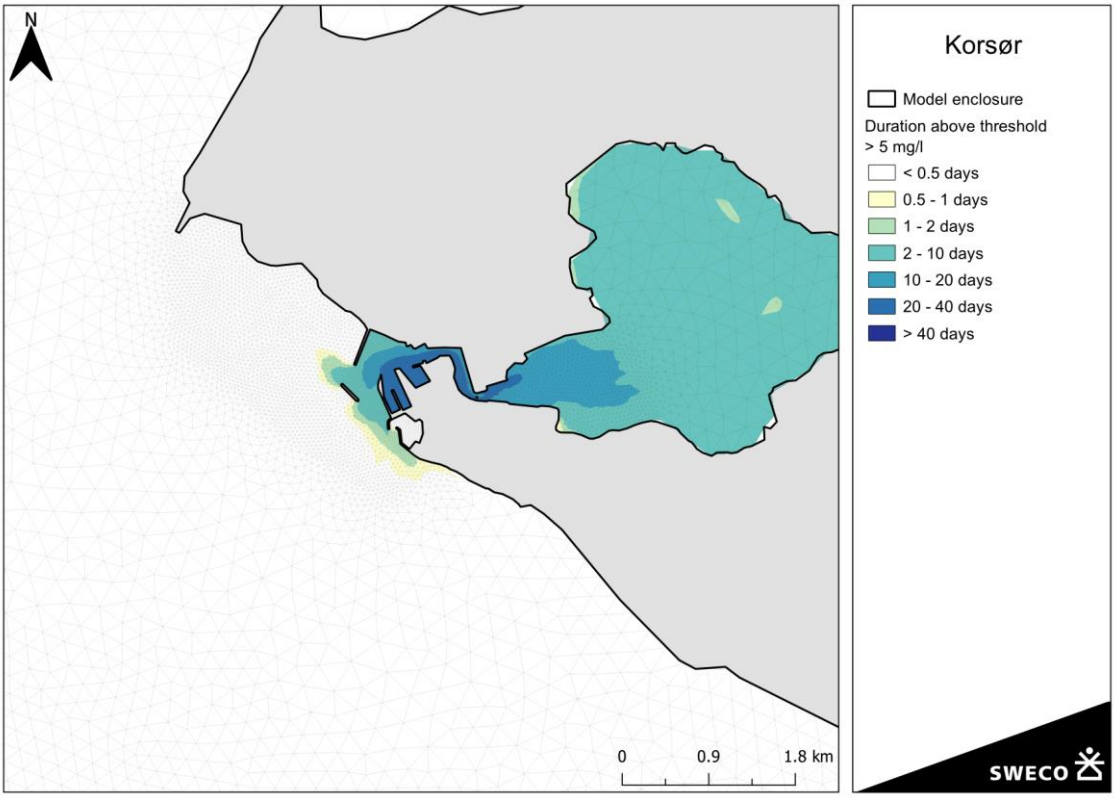

Figure 8.2: Model results without bubble curtain: Duration above 5 mg/l.

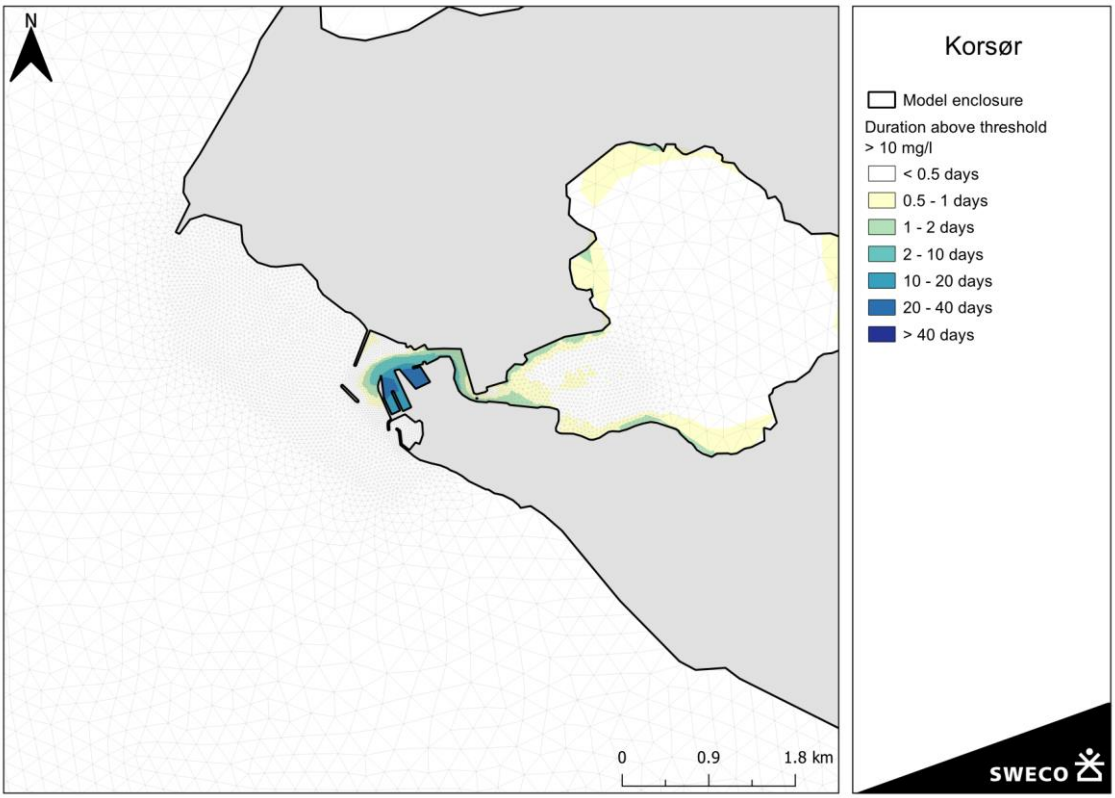

Figure 8.3: Model results without bubble curtain: Duration above 10 mg/l.

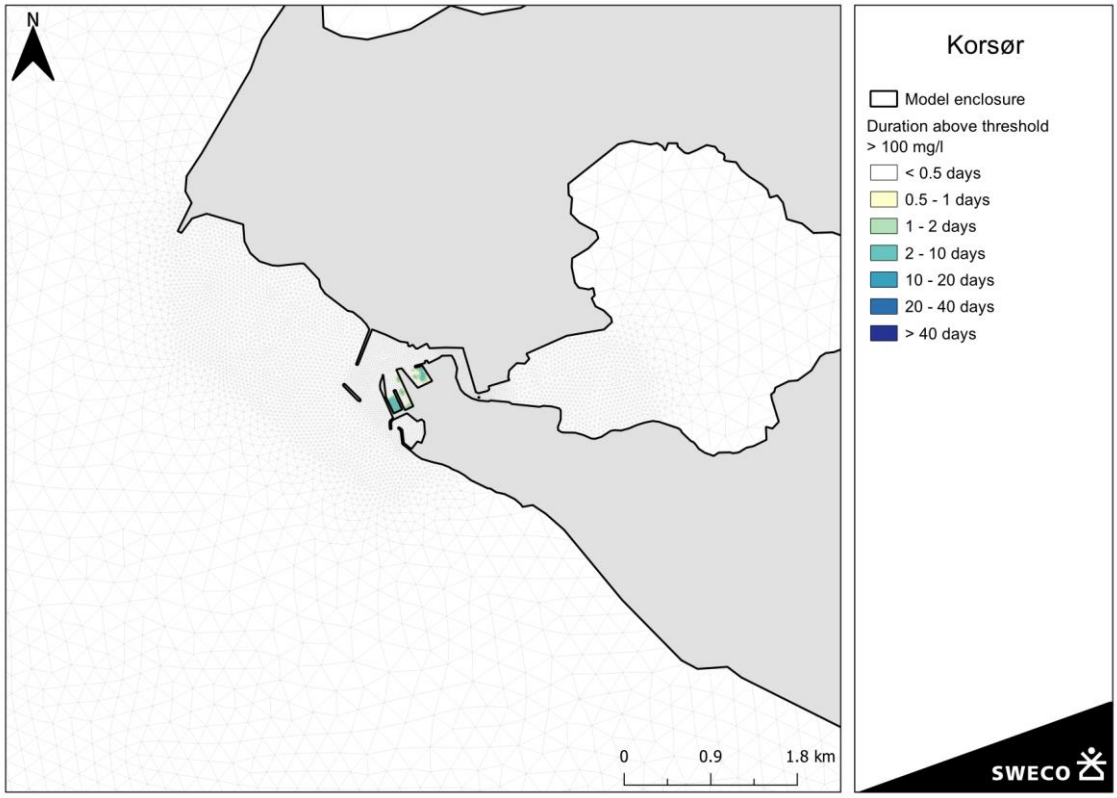

Figure 8.4: Model results without bubble curtain: Duration above 100 mg/l.

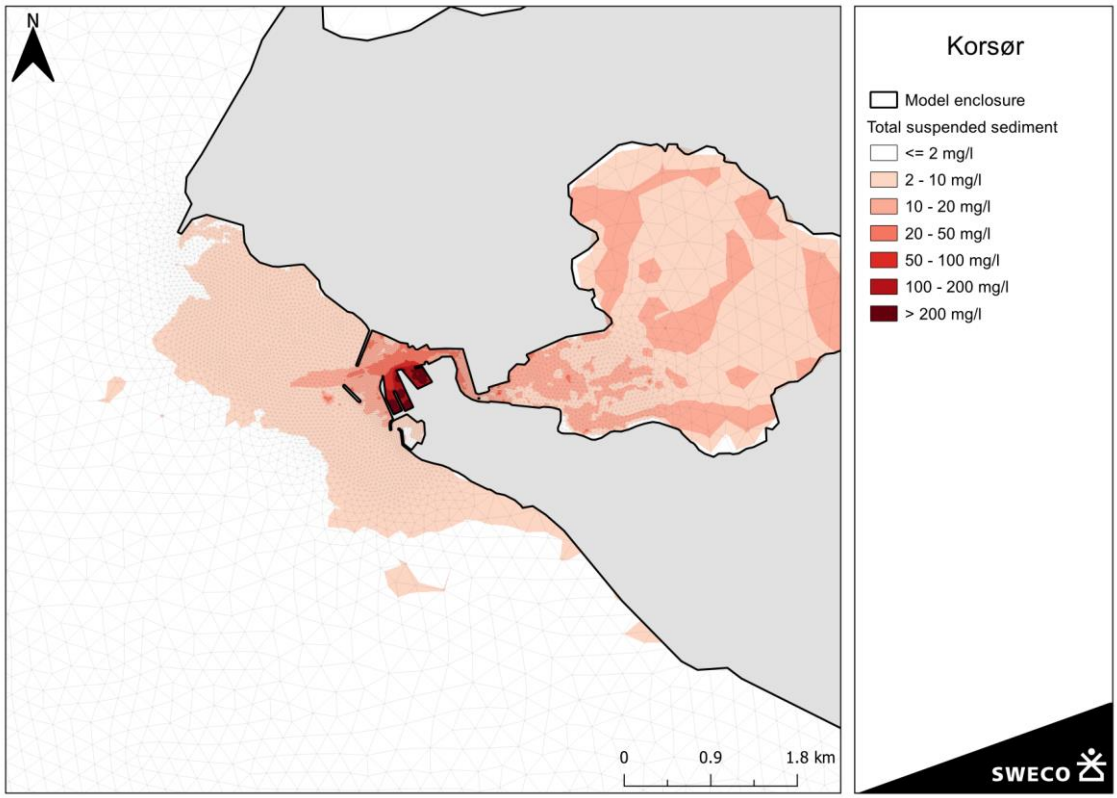

Figure 8.5: Model results without bubble curtain: Maximum concentration at bed.

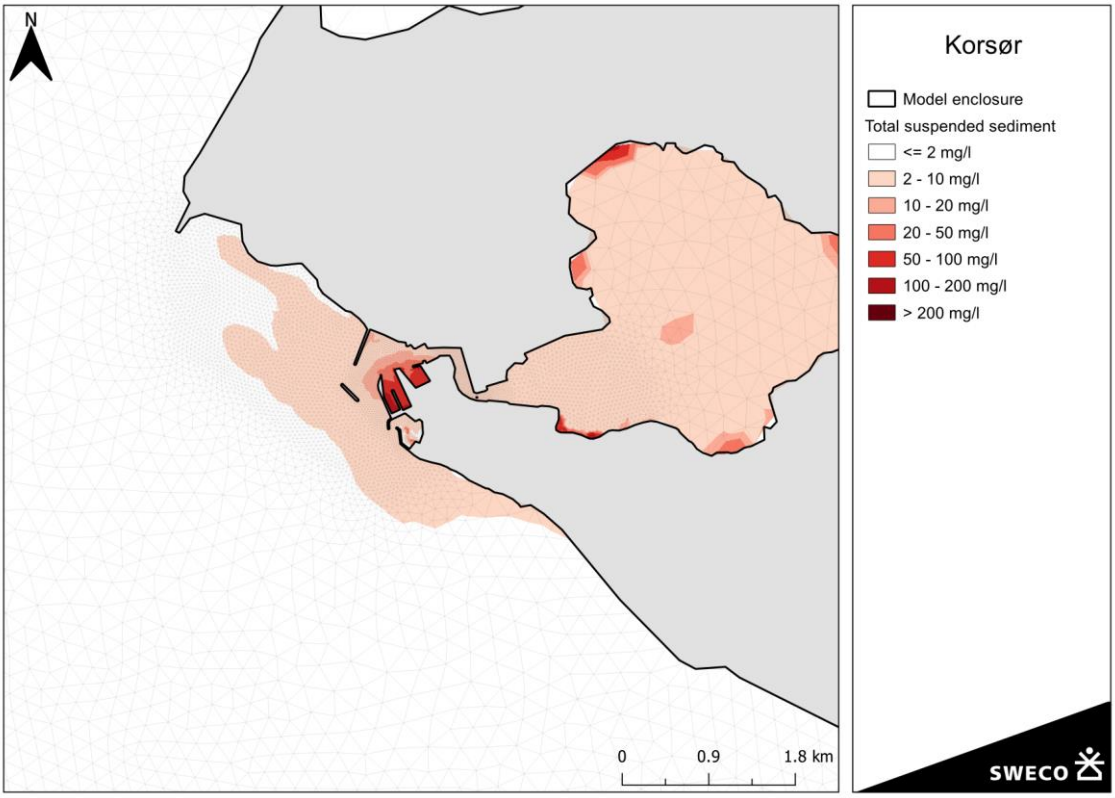

Figure 8.6: Model results without bubble curtain: Maximum concentration at surface.

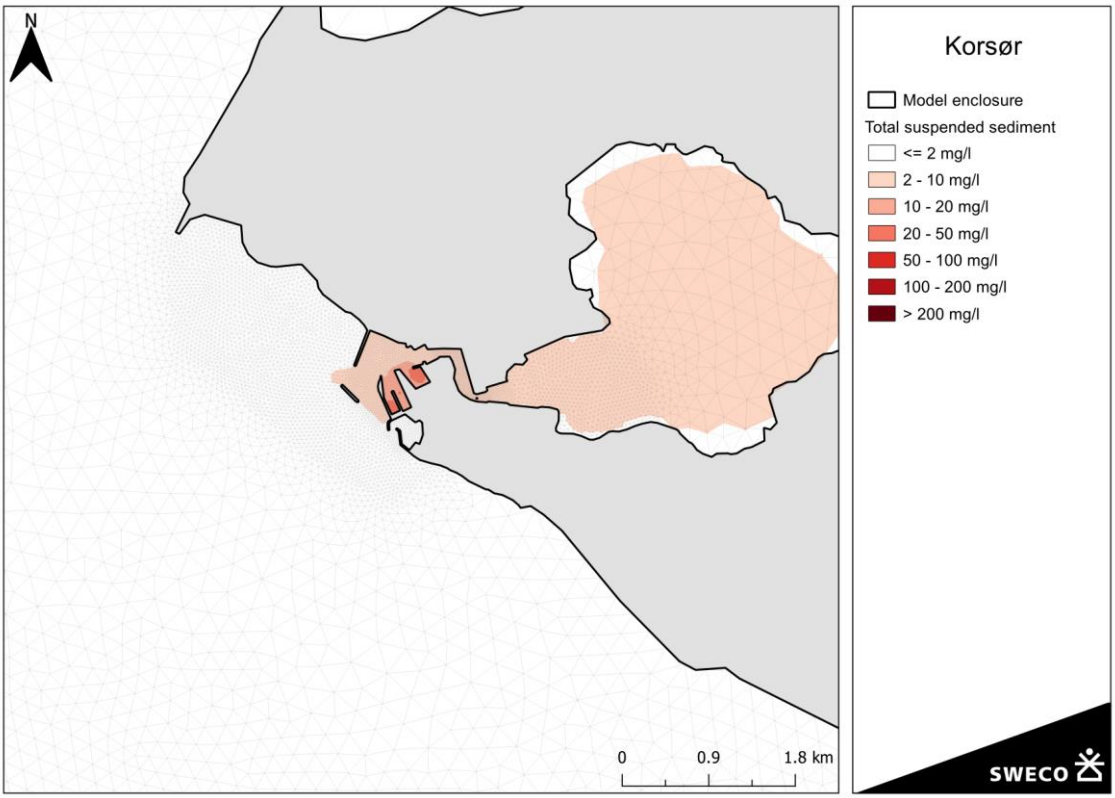

Figure 8.7: Model results without bubble curtain: Average concentration at bed.

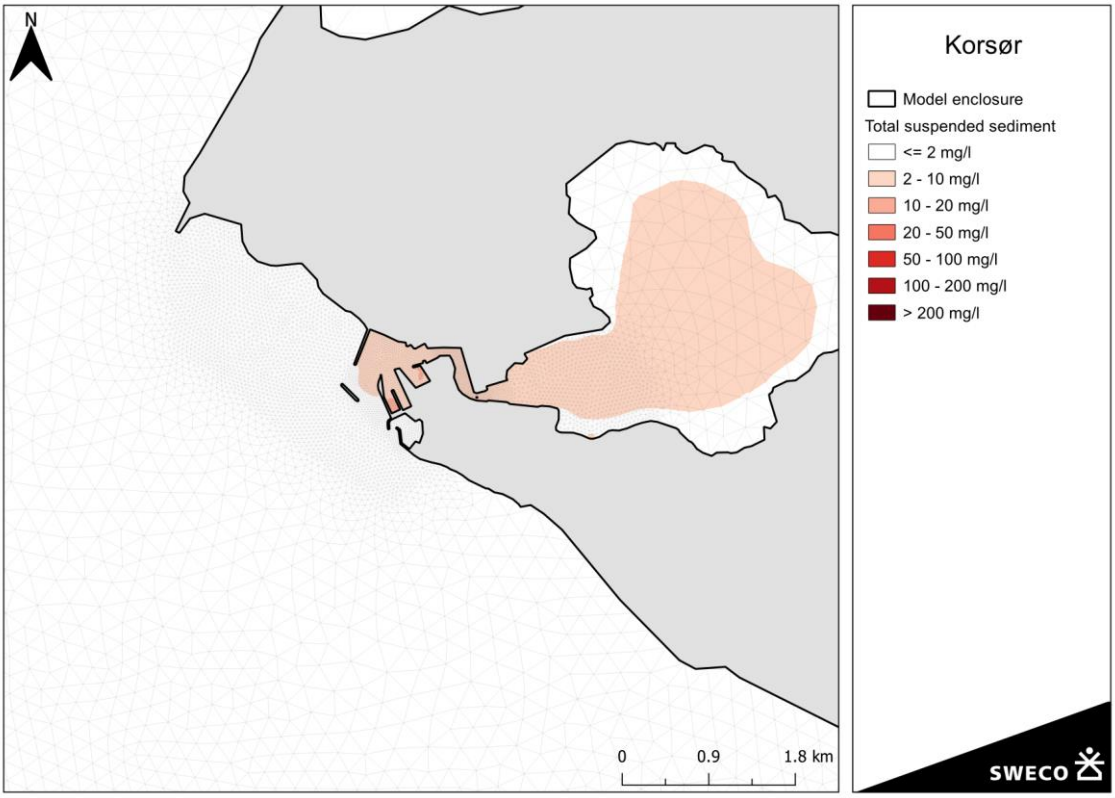

Figure 8.8: Model results without bubble curtain: Average concentration at surface.

C.2 Sediment deposition

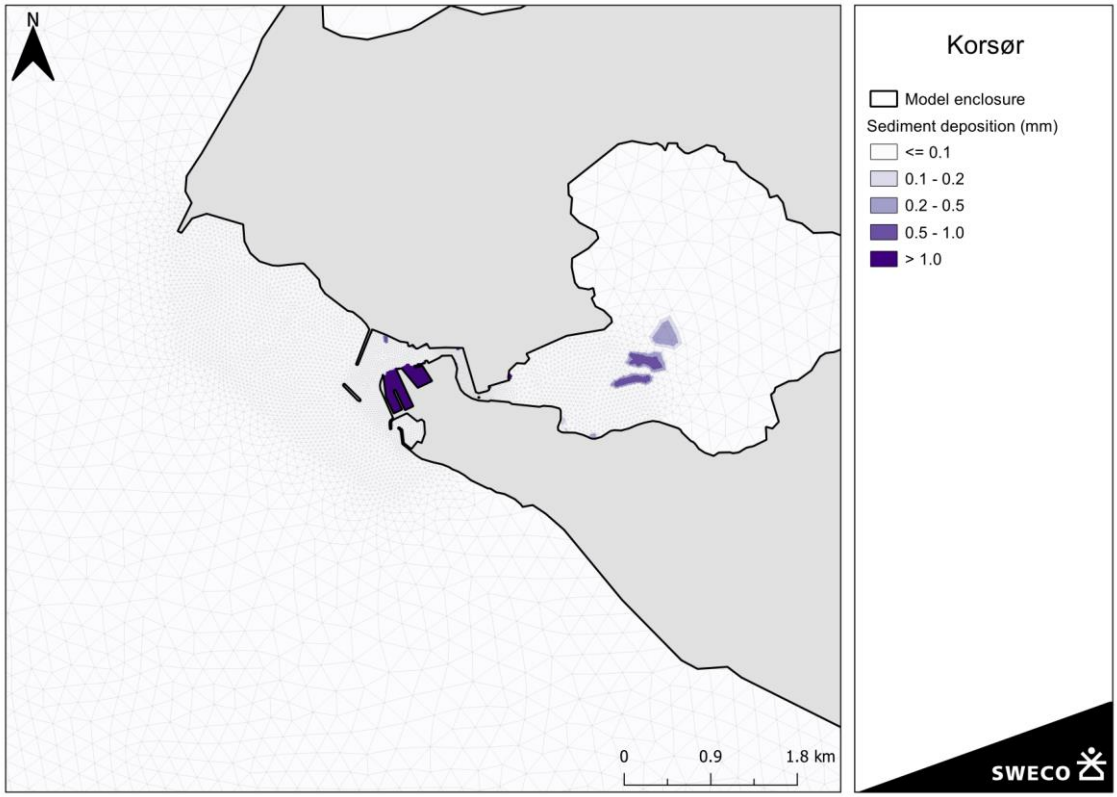

Figure 8.9: Model results without bubble curtain: Sedimentation.

C.3 Sediment deposition

Together with the release of sediment spill to the model, a tracer has been included in the dredging spill. The tracer is inert and stays in suspension for the entire simulation and is thus a conservative estimate. The results are used in the calculation of the spreading of nutrients in section 5.3.1.

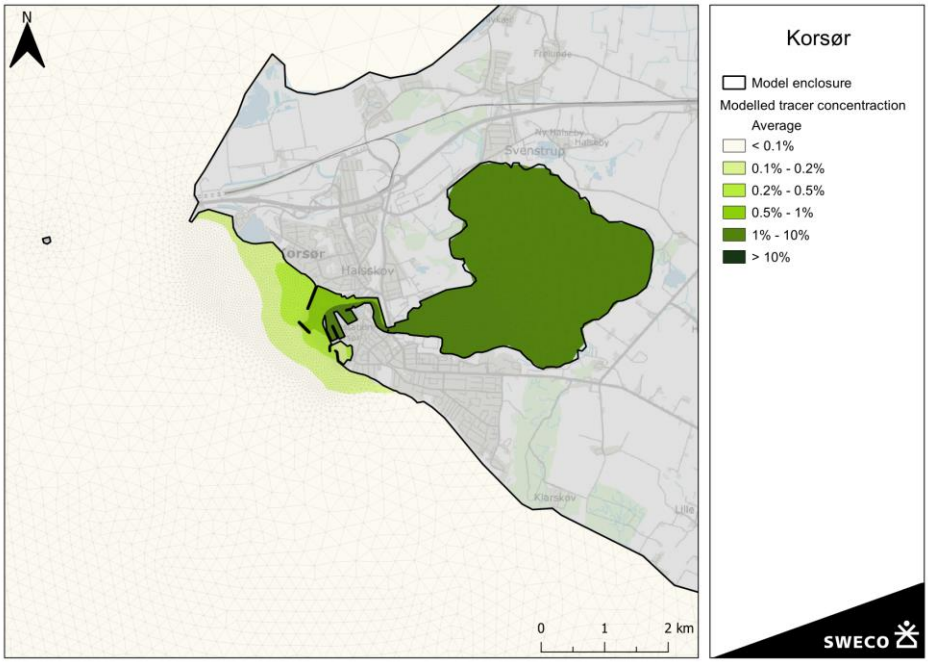

Figure 8.10: Inert tracer concentrations, relative to the concentration that is released at 1 m^3/s during the dredging hours. Average depth-averaged concentrations during the dredging period.

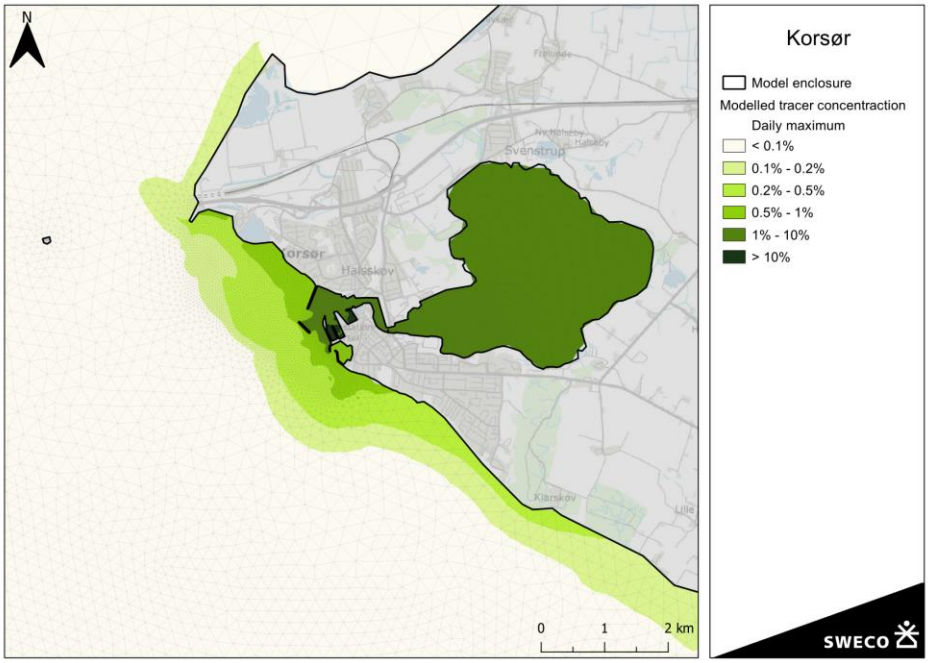

Figure 8.11: Inert tracer concentrations, relative to the concentration that is released at 1 m^3/s during the dredging hours. Maximum daily depth-averaged concentrations.